Original Article

Comparative Histological and Immunohistochemical Study of the Potential Protective Effects of Granulocyte Colony Stimulating Factor Versus Galangin on Induced Cardiac Toxicity in Adult Male Albino Rats

Hala El-Haroun[1,2], Nadia Said Badawy Khair[1], Eman Badawy Konsowa[1] and Mona Abd elmawla Soliman[1]

[1]*Department of Histology, Faculty of Medicine, Menoufia University, Egypt*

[2]*Department of Basic Medical Science, Faculty of Denistry, Al Ryada University for Science & Technology*

ABSTRACT

Introduction: Cardiomyopathy, which is distinguished by biochemical and histological alterations, significantly contributes to worldwide mortality, particularly ventricular infarction.

Objective: Is to assess histological alterations within the myocardium induced by Isoproterenol (ISP), and to explore the potential protective effects of Granulocyte Colony Stimulating Factor (G-CSF) versus Galangin.

Material and Methods: Sixty-six adult male albino rats were randomly assigned to four groups. Group I, control group (n=18), Group II: (n=16), received isoproterenol at a daily dose of 5mg/kg for 14 days; Group III (n=16) received Isoproterenol as in group II and G-CSF (at a dose of 10 µg/kg/day SC) for 6 days; and Group IV (n=16), received isoproterenol as in group II and Galangin at a dose of 1mg/kg for a duration of 4 weeks. At the end of the experiment, the animals were given anesthesia, euthanized, and cardiac samples were obtained for histological, immunohistochemical, and electron microscopic analysis.

Results: ISP treated group exhibited elevated concentrations of cardiac enzymes, specifically lactate dehydrogenase (LDH), creatine kinase MB isoenzyme (CK-MB), and cardiac troponin (cTn I). Additionally, a reduction in levels of antioxidant enzymes, including glutathione, SOD, and catalase was observed. Histological results included loss of myofibril bands, dark stained pyknotic nuclei, cellular infiltration, and extensive hemorrhage within widened endomysium. It also revealed increased area percentage of collagen, TNF-α, VEGF, and Caspase-3. Furthermore, ultrastructural observations revealed myofibril band disruption and fragmentation, swollen mitochondria and cracked Z-lines. These findings were ameliorated in group III and group IV but, the concurrent treatment of Granulocyte Colony Stimulating Factor (G-CSF) resulted in significantly more heart tissue preservation compared to Galangin.

Conclusion: G-CSF exhibits markedly more protective effect on cardiac tissue compared to Galangin on induced myocardial damage. More researches are needed to determine the protective effects and optimal dosage of G-CSF and galangin on humans to achieve greater efficacy.

Received: 26 January 2024, **Accepted:** 11 Feruary 2024

Key Words: Galangin, G-CSF, isoproterenol.

Corresponding Author: Eman badawy konsowa, MSc, Department of Histology, Faculty of Medicine, Menoufia University, Egypt, **Tel.**: +20 12 0558 0058, **E-mail:** eman.badwy14@gmail.com

ISSN: 1110-0559, Vol. 48, No. 1

INTRODUCTION

Worldwide, cardiovascular diseases constitute the primary cause of mortality. Myocardial infarction is the nation's most frequent manifestation of cardiovascular disease. Notwithstanding notable advancements in the management of acute myocardial infarction (MI) and coronary artery disease (CAD) over the past two decades, MI remains the primary etiology of heart failure (HF)[1]. Other researchers[2] recognized three unique clinical manifestations that differ in etiology, clinical characteristics, and prognosis based on the chronological evolution of MI onset and heart failure development. Myocardial necrosis or injury is the result of myocardial infarction. This condition is characterized by an elevation in cardiac biomarkers and supporting clinical evidence, including electrocardiogram (ECG) abnormalities, imaging confirmation of newly formed viable myocardium damage, or abrupt irregularities in regional wall motion[3].

The synthetic catecholamine isoproterenol has a beneficial impact on both the chronotropic and inotropic systems by acting as a β-adrenergic agonist. Consequently, a deficit arises between the augmented cardiac demand and the reduced coronary blood flow, which causes significant cardiac stimulation[4]. Furthermore, it is critical to specify that Isoproterenol (ISP) results in the generation of cytotoxic free radicals and reactive oxygen species (ROS). This procedure causes additional disruption to the intricate balance between antioxidative defense mechanisms and

DOI: 10.21608/ejh.2024.265643.2010

free radicals, thus bearing resemblance to MI that is observed in humans[5]. Additional scholars[6] hypothesized that the mechanism by which ISP induces Ca2+ influx stimulation is a crucial underlying factor that contributes to a variety of cardiac dysfunctions and, ultimately, myocardial damage. Granulocyte colony-stimulating factor (G-CSF) has been the subject of intense research and development over the past 20 years due to its potential as a crucial therapeutic intervention[7]. This glycoprotein is present in a wide variety of body tissues. It possesses the capacity to stimulate cell proliferation, mobilization, and survival[8]. It induces generation of diverse precursors, including stem cells and granulocytes, within the bone marrow, subsequently liberating into the circulation. It prevents pro-inflammatory cytokine production. G-CSF suppressed TGF-1 expression through the generation of anti-fibrogenic cytokines. G-CSF therapy decreased interleukin-6, TGF-b1, and collagen type IV mRNA levels[9]. It has been demonstrated that G-CSF stabilizes myocardial electrophysiological characteristics, prevents ventricular remodeling, decreases the risk of ventricular arrhythmia during ischemia reperfusion injury, and inhibits myocardial apoptosis and inflammation[10].

Galangin, which is a polyphenolic compound (3,5,7-trihydroxyflavone or 3,5,7-trihydroxy-2-phenyl-4H-chromen-4-one), is derived from the galangal ginger plant. Honey, lesser galangal, and greater galangal plants are all abundant in Galangin. Traditional medicine has utilized "propolis" a bee glue that is abundant in Galangin, to treat wounds, sores, and swelling[11]. Galangin has been demonstrated in prior studies to inhibit cell proliferation, stimulate apoptosis, impede cell metastasis, stimulate cell autophagy, and exhibit anti-inflammatory as well as antioxidant characteristics[12]. According to recent research, it is of paramount importance in the progression of neointimal hyperplasia subsequent to vascular injury[13]. Galangin has been associated with several beneficial biological impacts, including antibacterial, anticancer, anti-apoptotic, antifibrotic, and anti-inflammatory characteristics[14]. Galangin enhanced the activity of autogenous antioxidant enzymes, such as SOD, CAT, glutathione peroxidase, and glutathione-S transferase, thereby mitigating oxidative damage[15].

For simulating myocardial ischemia, the ISP-induced model is a straightforward, non-invasive, time-efficient, and economical method that maintains the pericardium's integrity and necessitates only minor surgical intervention. As stated earlier, the administration of ISP consistently leads to cardiac dysfunction with dilatation of the left ventricle, resembling the symptoms observed in the extensively infarcted heart[16]. In our investigation, myocardial infarction (MI) was provoked through subcutaneous isoproterenol (ISP) administration[6].

The aim of this scientific investigation is to evaluate the histological consequences of Galangin versus G-CSF on cardiotoxicity induced by isoproterenol.

MATERIAL AND METHODS

Ethical approval

Following the guidelines for animal care established by the National Institutes of Health (NIH), the Faculty of Medicine at Menoufia University granted Institutional Research Board (IRB) approval for this study (Code number: 2/2022 HIST 48).

Animals

The experiment utilized 66 twelve-weeks-old adult male albino rats weighing 170–200 grams. The University of Menoufia Faculty of Medicine's animal facility supplied the study's animals. They got one week to adjust to the lab before the experiment. The animals had unrestricted consumption of water and food at ambient temperature in safe, conventional cages. and their general health was assessed.

Chemicals

G-CSF: G-CSF-filgrastim (recombinant human granulocyte-colony stimulating factor 300 µg/ml liquid for systemic or intravenous injection) was supplied by SEDICO Pharmaceuticals Company (Egypt). It was purchased from El-Ezaby pharmacy, Egypt.

Isoproterenol hydrochloride: it was purchased from Sigma-Aldrich Co., St. Louis, MO, USA in the form of powder. The powder was liquified in normal saline. It was given to the animals via subcutaneous injection.

Galangin: it was purchased on line from Nine-life web site in the form of powder. The powder was purified to 99.24% by Medical S&T Development (Shanghai, China). It was dissolved in corn oil and given orally to rats by gastric tube.

Experimental procedure

The animals were randomly grouped into four groups.

Control Group I (18 rats) was assigned at random to the following five subgroups:

- Subgroup Ia: 3 animals remained untreated for the duration of the experimental period (4 weeks).
- Subgroup Ib: 3 rats subcutaneously injected by 1 ml of normal saline daily for 14 days (vehicle for ISP)
- Subgroup Ic: 4 rats were orally administered 1 ml of corn oil (vehicle for Galangin) orally once daily during the period of experiment.
- Subgroup Id (G-CSF treated group): 4 rats obtained G-CSF therapy. The rats were given Filgrastim (G-CSF) at a daily rate of 10 µg/kg/day SC over 6 days[17] before being left untreated for the duration of the trial (4 weeks).
- Subgroup Ie [Galangin-treated group]: 4 rats were given galangin at a dose of 1mg/kg b. wt.[14] once a

day for 4 weeks via an intragastric tube. Galangin powder dissolved in corn oil.

Group II [Isoproterenol (ISP) treated] (n=16): subcutaneous injections of ISP at a dosage of 5mg/kg b. wt. daily for 14 days were administered to these rats[14].

Group III [G-CSF & Isoproterenol treated] (n=16): For a duration of six days, 16 rats were subcutaneously injected with Filgrastim (G-CSF) at a rate of 10 µg/kg/day[17] then, subcutaneous injection of ISP as described earlier[14].

Group IV [Galangin & Isoproterenol treated group] (n=16): Galangin was administered orally to 16 rats as described for four weeks prior to each isoproterenol subcutaneous injection for 14 days as described[14].

Rats were weighed 24 hours after their last medication treatment, and blood samples were drawn from tail veins using heparinized capillary tubes to determine serum levels of cardiac enzymes. The rats were subsequently anesthetized with an intraperitoneal intake of 100 mg/kg ketamine-xylazine[18]. The rats were slaughtered. Their hearts were removed, cleaned, and weighed using an electronic scale in grams. After being excised, the specimens were immersed in normal saline. The tissues were split, and histological investigations were conducted.

Biochemical assessment

All biochemical investigations were carried out in the central lab. Menoufia University's Faculty of Medicine.

Serum cardiac marker enzymes

Levels of cardiac troponin I (c TnI), creatine kinase-MB (CK-MB), and lactate dehydrogenase (LDH) were measured to assess cardiac muscle damage[19].

Oxidative stress markers

- Estimate malondialdehyde (MDA) to indirectly detect lipid peroxidation. MDA was quantified in nmol/mg protein as per Milinković-Tur et al.[20].
- Superoxide dismutase (SOD) activity was estimated in supernatant fractions using Zammel *et al*.'s approach (unit protein/mg protein)[21].
- Catalase (CAT) activity, use a molar extinction coefficient of 43.6x103 M-1 cm per unit protein (mg protein)[22].
- Reduced glutathione (GSH) estimation: activity of reduced GSH were expressed as mmole/mg protein using Ganesan *et al*.[23] technique.

Light microscopic studies

Histological study

Dissected cardiac muscle from the left ventricle apex was fixed in 10% formol saline, dehydrated, processed, and embedded in paraffin wax. To analyze the heart muscle architecture, 5 µm thick slices were stained with Hx&E and to identify collagen fibers the Mallory's Trichrome stain was done[24].

Immunohistochemical staining

Anti- Caspase-3 antibody (apoptotic marker): (Thermo Scientific, Fermont, California, USA; anticaspase-3 rabbit polyclonal antibody, dilution 1:200). The characteristics of the reaction were cytoplasmic and nuclear[25]. A Section of human tonsil was utilized as positive control.

Tumor necrosis factor-alpha (TNF-α) (index of inflammation): Primarily, a mouse anti-TNF-α antibody (Santa Cruz Biotechnology, California, USA, dilution 1:100) was utilized as the monoclonal antibody. The site of the reaction was the cytoplasm[26]. The liver served as a positive control for TNF-α.

Vascular endothelial growth factor (VEGF) (an indicator of neovascularization): A primary antibody that targets VEGF and is monoclonal to mice was utilized (Thermo Scientific and Lab Vision Corporation, CA 94539, USA, dilution 1:20). The pattern of cytoplasmic staining for VEGF was identified[27]. kidney was used as a positive control for VEGF.

Negative controls were generated using the same method; however, they did not contain the main antibody. Mayer's hematoxylin was used to counterstain all immune-stained sections.

Transmission Electron Microscopy (TEM)

Thin slices (1x1mm) of left ventricle apex were cut and immediately fixed for 3 hours at 4°C in 3% glutaraldehyde buffer at PH 7.4, dehydrated, and fixed with 1% osmium tetroxide for 2 hours before embedding in epoxy resin. Uranyl acetate and lead citrate-stained copper grid-produced ultrathin cardiac slices (70-90 nm). Using a JEM-1400 plus electron microscope, tissue ultrastructure was examined. TEM images were processed and analyzed by Alexandria University's Faculty of Science Electron Microscopy Unit[28].

Morphometric analysis

All quantitative data were acquired using Image J's Image analyzer program version K1.45. Ten non-overlapping randomly selected fields from each slide of each group were quantified. The data were measured using H&E, Masson's Trichrome, and immunohistochemistry. These illustrated parameters were calculated for quantitative evaluation:

- The average area percentage of collagen fibers in sections stained with Masson's Trichrome (x 400).
- Mean percentage of caspase 3 immuno-positive reaction in immuno-stained sections (× 400).
- Mean area percentage of TNF-α immune-positive reactivity in stained sections (×400).
- Mean area % of VEGF immuno-positive reaction in VEGF immuno-stained sections (× 400).

Statistical analysis

The results for body weight (g), heart weight (g), biochemistry, and morphometry were provided as mean ± standard deviation. The analysis of the data was carried out using SPSS version 20 (Chicago, Illinois, USA). For comparison between groups, a one-way ANOVA was utilized, subsequent to a least significant difference (LSD) post-hoc test. *P-values* < 0.05 were considered significant[29].

RESULTS

General observations

Control subgroups had identical general conditions, biochemical, histological, and immunohistochemical data, hence they were grouped together as control group (I). Control animals (group I) were healthy, having typical nutritional consumption, activity, and development. The ISP-treated group (II) had lower weight, appetite, and physical activity. Throughout the experiment, many animals were ill and feeble, and three animals from this group have died. Compared to the ISP-treated group, animals given G-CSF (group III) or Galangin (group IV) with ISP had a normal appetite and were healthier than the ISP-treated animals.

Regarding Body weight

The ISP-treated group (II) exhibited a significantly reduced body weight (P<0.001) than the control group. There was no significant difference in body weight (p > 0.05) between the control group (I) and Group III, which received ISP and G-CSF. Group IV treated with ISP and Galangin had a significantly less body weight (p<0.05) compared to the control group. Compared to the ISP-treated group (group II), the Galangin-treated group (group IV) had a significant rise in body weight (p <0.05). The ISP and Galangin-treated group (IV) body weighted substantially less (p < 0.05) than the ISP and GCSF group (III). All these data were documented in (Table I, Histogram 1).

Regarding heart weight

The ISP-treated group (II) exhibited considerably increased heart weight (P<0.001) compared to the control group. While the heart weight of group III, which received ISP and G-CSF, did not differ substantially from the control group (p > 0.05). Group IV treated with ISP and Galangin had significantly greater heart weight (p<0.05) compared to the control group. Compared to group II, animals in the ISP and G-CSF-treated group (III) had considerably lower heart weights (p<0.05). Rats treated with ISP plus Galangin (IV) had considerably lower heart weight (p > 0.05) than group II treated with ISP alone. The ISP and Galangin-treated group (group IV) exhibited considerably increased heart weight (p < 0.05) compared to the ISP and GCSF group. All of these data have been recorded in (Table I, Histogram 2).

Biochemical results

Serum Cardiac Marker Enzymes

The ISP-treated group (II) had significantly greater serum enzyme levels (p<0.001) than the control group. The ISP and GCSF-treated rats (III) showed the same serum levels of cardiac enzymes as the control group (p > 0.05). Serum levels of CK-MB, cTnI, and LDH were considerably higher (p<0.05) in the ISP and Galangin-treated group (IV) than the control. In group III, ISP plus GCSF treatment significantly reduced serum cardiac enzyme levels (p<0.05) compared to ISP-treated group II. Group IV received ISP-plus-Galangin showed a substantial decrease (P < 0.05) compared to group II. Serum levels of CK-MB, cTnI, and LDH showed significant increase (p < 0.05) between ISP and Galangin (group IV) and ISP and GCSF (group III). All these data were recorded in (Table I, Histograms 3,4).

Lipid peroxidation and antioxidant enzymes

The ISP-treated group (group II) showed considerably greater plasma MDA levels (a measure of lipid peroxidation) than the control group (p<0.001). The ISP and GCSF-treated groups (III) showed no difference from the control group (p > 0.05). In contrast, rats treated with ISP and Galangin (group IV) showed a substantial increase (p< 0.05) compared to the control group. In comparison to the ISP and GCSF group (group III), the ISP and Galangin-treated group (group IV) showed a substantial rise (p < 0.05) in serum MDA levels.

The ISP-treated group (II) had significantly lower plasma antioxidant enzyme levels (p<0.001) than the control group. The ISP and GCSF groups (group IV) showed no significant change from the control group (p > 0.05). However, rats treated with ISP and Galangin (group IV) showed a substantial reduction (p<0.05) compared to the control group. Serum antioxidant enzyme levels were significantly higher (p<0.05) in group III treated with ISP plus G-CSF than in group II treated with ISP. However, group IV treated with ISP and Galangin showed no statistically significant increases (p > 0.05) in serum antioxidant levels as compared to group II. Compared to ISP and GCSF-treated group III, serum antioxidant enzyme levels in the ISP and Galangin-treated group (group IV) decreased significantly (p < 0.05). All these data were set in (Table 2, Histogram 5.

Light Microscopic (LM) and Morphometric Results

Hematoxylin and Eosin Stain

Group I (Control group): The myocardium of the left ventricular wall of the control animals exhibited normal histological architecture of the heart muscle in longitudinal sections. It had branching, interconnected striated muscle fibers with a delicate connective tissue endomysium including fibroblasts surrounding the cardiac muscle fibers. The striated muscle fibers had single centrally situated pale oval basophilic nucleus and acidophilic sarcoplasm.

Transverse striations and intercalated discs between cardiomyocytes were observed as well (Figure 1A).

Group II (ISP-treated group): This group's left ventricular wall myocardial sections demonstrated a lack of normal cardiac muscle fiber architecture. There were also certain areas of complete loss of some fibers, as well as darkly stained pyknotic nuclei. Additionally, the widening of the endomysium revealed extravasation and a significant hemorrhage (Figures 1 B1,B2,B3,B4). Significant vacuolation and cellular infiltration was also observed (Figures 1 B3,B5).

Group III (ISP+ G-CSF): This group's left ventricular wall myocardial sections displayed a full restoration of the typical myocardial structure with centrally placed pale oval vesicular nuclei. The fibroblast nuclei were also shown to be flattened. Intercalated discs connect cardiomyocytes (Figure 1C).

Group IV (ISP+ Galangin): This group's left ventricle wall myocardial sections displayed a moderate restoration of the normal myocardial structure. However, some pyknotic nuclei, widened endomysium, vacuoles, and focal hemorrhagic areas have been identified (Figure 1D).

Mallory's Trichrome Stain

Group I: Regarding Mallory Trichrome-stained sections of control rats' myocardium, the endomysium contained the least quantity of collagen fibers (Figure 2A).

Group II (ISP-treated group): ISP-treated rats' myocardial sections revealed extensive collagen fiber deposits within the endomysium and the surrounding blood vessels (Figure 2B). When contrasted with the control group, the mean area percentage of collagen fibers in this group's sections revealed a significant rise ($P < 0.001$). (Figure 2 H6, Table 3).

Group III (ISP + G-CSF group): This group's myocardial sections indicated a low concentration of collagen fibers within the endomysium and surrounding blood vessels (Figure 2C). The mean area percentage of collagen fibers was not statistically differed comparable from the control ($P>0.05$), but significantly lower than the ISP-treated group ($p<0.001$) (Figure 2 H6, Table 3). Group IV (ISP + Galangin): Rats demonstrated a little increase in collagen in their endomysium in myocardial sections (Figure 2D). The mean area percentage of collagen fibers was substantially lower ($P < 0.05$) than in rats receiving ISP (group II), but significantly greater ($P < 0.05$) than in those who were administered with Isoprotrenol + G-CSF (III) (Figure 2 H6, Table 3).

Immunohistochemical study

Caspase-3

Group I (control): Caspase-3 immunohistochemistry staining of this group's rats' myocardium revealed a negative sarcoplasmic immune response (Figure 3A).

Group II (ISP -treated rats): The group demonstrated a marked positive sarcoplasmic immunoreaction (Figure 3B). This group had a considerably greater mean area percentage of caspase-3 positive immunoreaction ($p<0.001$) than the control group. (Figure 3 H7, Table 3). Group III (ISP + G-CSF): This group of rats' myocardia was immunohistochemically stained for Caspase-3, which demonstrated a minor sarcoplasmic response (Figure 3C), with no statistically significant alteration ($P>0.05$) contrasted with the control group, but a significant decline in area% ($p<0.001$) when compared to the ISP-administered group. (Figure 3 H7, Table 3).

Group IV (ISP + Galangin): In this group of rats, Caspase-3 immunohistochemical labeling of the myocardium showed notable sarcoplasmic immunological reactivity (Figure 3D), with a substantial ($P < 0.05$) increase in mean area% relative to the control. In relation to the ISP and GCSF-treated groups, there was a statistically significant increase ($P < 0.05$). (Figures 3 H7, Table 3).

Tumor necrosis factor (TNF-α)

Group I (control): TNF-α Immunohistochemical staining of the myocardium of rats in this group revealed negative immunological expression (Figure 4A).

Group II (ISP)-treated): Rat myocardium exhibited a robust positive nuclear immunological response when stained with TNF-α (Figure 4B). Compared to the control group, the mean area% increased significantly ($P < 0.001$) (Figures 4H8, Table 3).

Group III (ISP + G-CSF): Myocardial sections from this group exhibited mildly positive immunological expression (Figure 4C). The area percentage of TNF-α in G-CSF and ISP treated groups indicated no statistically significant distinction ($P > 0.05$) from the control, but a substantial decline ($P < 0.001$) in relation to the ISP treated group. (Figures 4H8, Table 3). Group IV (ISP + Galangin): Myocardial sections from this group exhibited somewhat high immune expression (Figure 4D). ISP and Galangin administration substantially raised TNF-α area% ($P < 0.05$) in contrast to the control group. The ISP and Galangin-treated groups significantly increased the area percentage of TNF-α immunostaining ($P < 0.05$) relative to the ISP and GCSF-treated groups. (Figures 4H8, Table 3).

Vascular endothelial growth factor (VEGF)

Group I: Immunohistochemical stain for vascular endothelial growth factor (VEGF) demonstrating limited positive cytoplasmic immunoreaction in endothelial cells lining the blood vessels (Figure 5A).

Group II (ISP-treated): This group's cardiac sections exhibited a high positive cytoplasmic immunoreaction within blood vessel-lining endothelial cells (Figure 5B). The VEGF immunohistochemistry stain showed a substantially higher mean area percentage of VEGF ($P<0.001$) relative to the control (Figure 5H9, Table 3).

Group III (ISP + G-CSF): The immunohistochemical stain for VEGF revealed a slight positive cytoplasmic immunoreaction (Figure 5C) with a lack of significance ($P>0.05$) with regard to the control. (Figures 5H9, Table 3).

Group VI (ISP + Galangin): The VEGF immunohistochemistry labeling demonstrated a relatively high cytoplasmic immunoreaction (Figure 5D), which was significantly greater than in the control and ISP +G-CSF groups ($P < 0.05$), but greatly reduced ($P < 0.05$) when compared to the ISP group. (Figures 5H9, Table 3).

Transmission Electron Microscopic Results

Control group (1): The myocardium of the control group from the left ventricle wall revealed that the cardiomyocyte had an euchromatic central nucleus and was packed with well-organized parallel myofibrils, and numerous normal mitochondria placed between them and in the perinuclear region (Figure 6). The Z-line bisected the light I bands, while the H-zone bisected the dark A bands, revealing rows of mitochondria between them (Figure 7). Nevertheless, a regular intercalated disk was seen (Figure 8).

Group II (ISP-treated group): The myocardium of this group had an irregularly indented nucleus with peripherally condensed marginated chromatin, swollen mitochondria, and a disturbance in the banding pattern of the myofibrils (Figure 9). In addition, fragmentation, and disruption of the banding pattern of myofibrils were detected (Figure 10). There was severe disorder and loss of the typical myofibril arrangement with the existence of disturbed areas (Figures 11,12), whereas others had complete lysis (Figure 12). Many vacuoles were also, seen (Figure 11). Numerous mitochondrial damages were observed (Figures 9,10, 11). Furthermore, many glycogen granules were seen in between the deteriorated myofibrils (Figure 12). T-tubule dilatation was observed, as well as a region with broken Z-lines (Figure 13). The intercalated disc, on the other hand, featured areas of deformation and extreme disorder (Figures 11,14).

Group III (ISP+ G-CSF treated group): This group's cardiomyocytes had an euchromatic nucleus (Figure 15), nearly consistently distributed myofibrils with rows of mitochondria in between more or less as in control group (Figures 15,16), and dark A and light I bands alternating on their myofibrils. This group's myocardium also had a generally normal T-tubule (Figure 16) and an intact intercalated disc (Figure 17).

Group IV (Isoproterenol + Galangin) treated group: This group's cardiomyocytes had an irregularly indented nucleus with peripherally condensed chromatin and nearly regularly distributed myofibrils, but there were still areas of myofibril and Z-line degeneration. Furthermore, numerous mitochondria were found encircling the myofibrils and in the perinuclear area. (Figure 18). There was also an intercalated disk with deformed areas (Figure 19).

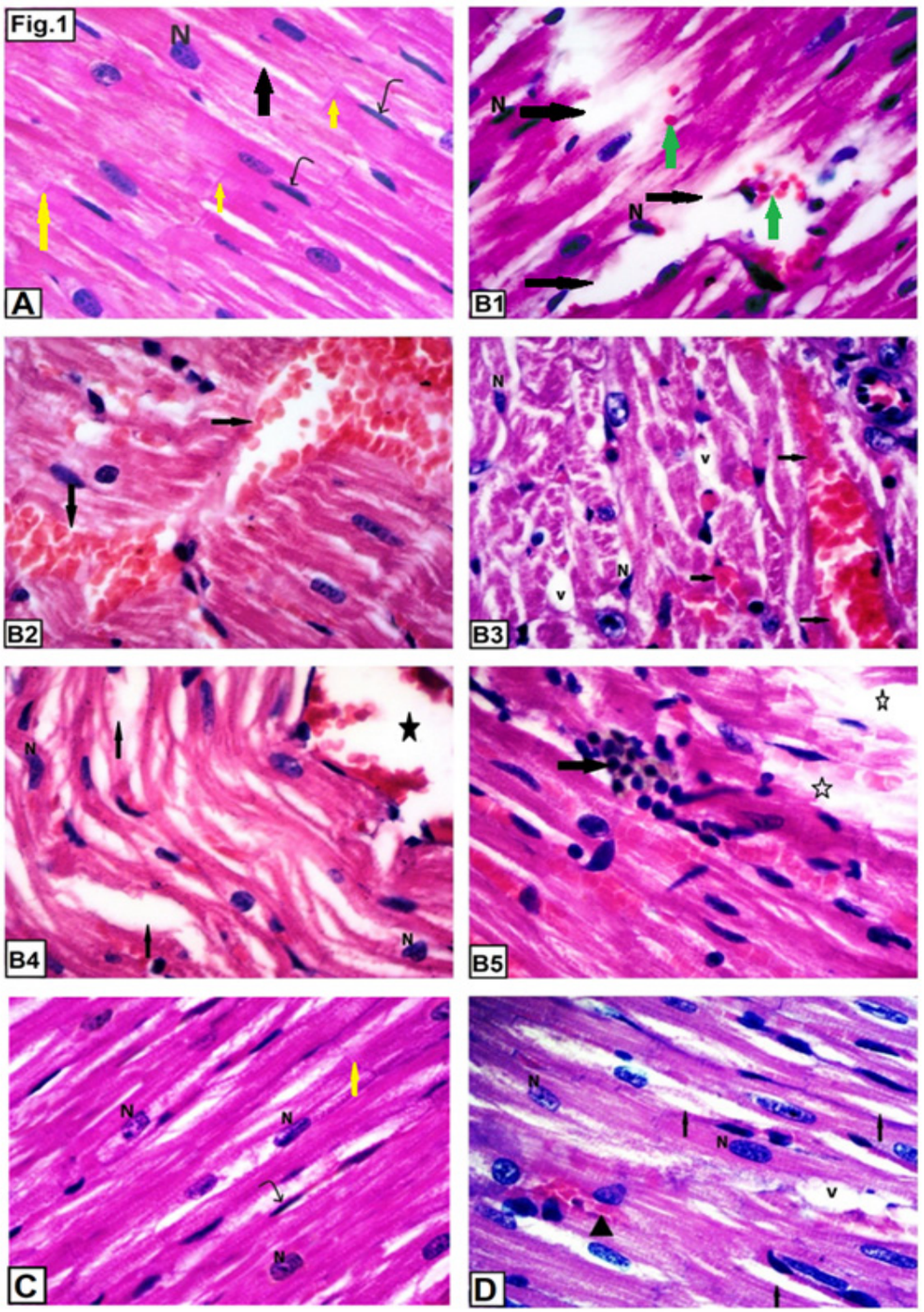

Fig. 1: A photomicrograph of a longitudinal section of the myocardium (A) Group I: exhibiting branching cardiac muscle fibers with centrally placed oval nuclei (N) and acidophilic sarcoplasm. There are Intercalated discs (yellow arrows) and connective tissue endomysium (black arrows), containing fibroblast with flattened nuclei (curved arrow). (B1) Group II (ISP treated group) demonstrating loss of normal cardiac muscle fiber architecture with wide areas of complete loss of cardiac fibers (black arrows) with darkly stained pyknotic nuclei of cardiomyocytes (N). Extravasated RBCS (green arrow) is also seen. (B2) Group II (ISP treated group) demonstrating extensive hemorrhage (arrows) within widened endomysium. (B3) Group II (ISP treated group) exhibiting fragmented, degraded muscle fibers with darkly stained nuclei (N) and vacuolated areas (V) and hemorrhagic spots between muscle fibers (arrow). (B4) Group II (ISP treated group) reveals areas with complete loss of muscle fibers (arrows) and darkly stained pyknotic nuclei (N). A congested blood vessel is also visible (star). (B5) Group II (ISP treated group) showing disfigured muscle fibers with localized areas of complete muscle fiber loss (star). Cellular invasion is evident (arrow). (C) Group III (ISP + G-CSF group): demonstrating almost normal cardiac muscle fibers with centrally placed pale oval nuclei (N). Intercalated discs (yellow arrow) link cardiomyocytes. Flattened fibroblast nuclei are also visible (curved arrow). (D) Group IV (ISP + Galangin group): demonstrating relatively normal cardiac muscle fibers with centrally placed pale, and vesicular nuclei (N). The endomysium has been expanded (arrows). There are vacuoles (V) and hemorrhagic spots (arrowhead). (Hx& E × 400)

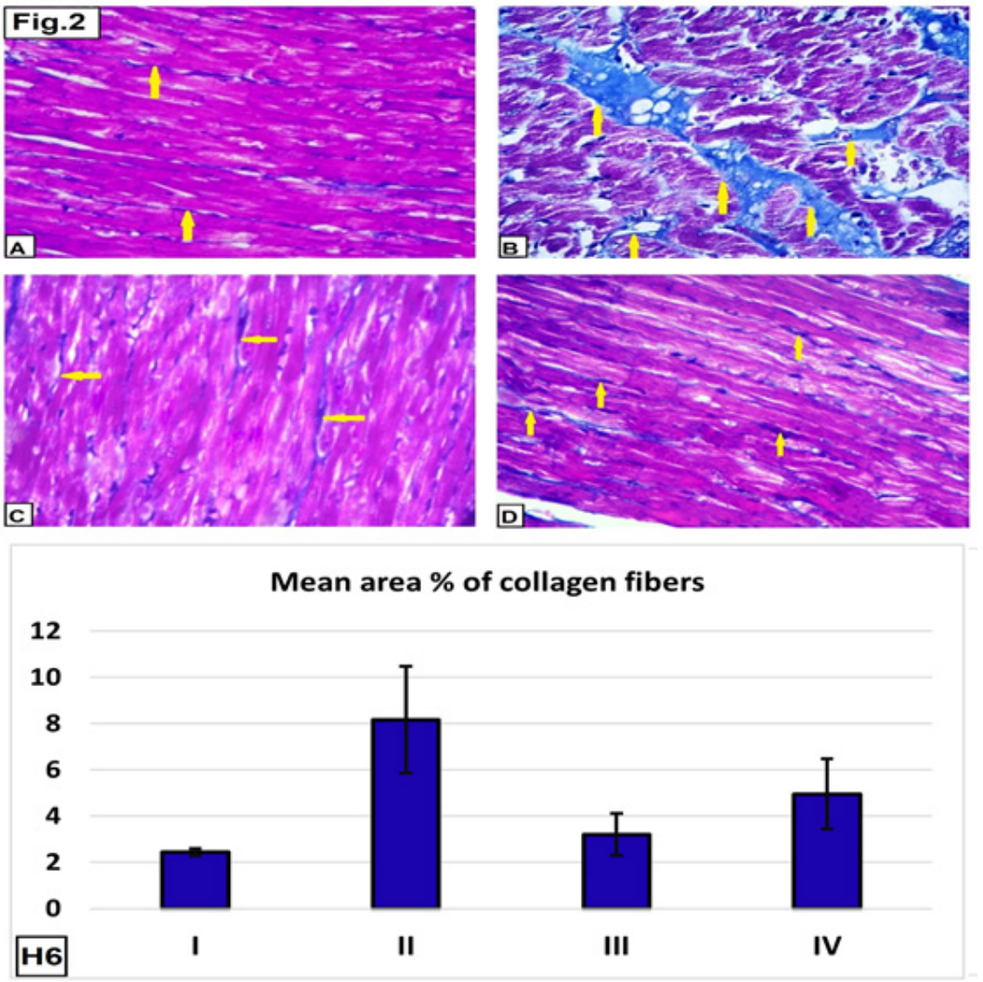

Fig. 2: A photomicrograph of a longitudinal section of the myocardium A) Group I: demonstrating minimal amount of collagen fiber distribution within endomysium (arrows). B) Group II demonstrating extensive collagen fiber deposition within endomysium (arrows). C) (ISP + G-CSF group): demonstrating presence of a few collagen fibers within the endomysium (arrows). D) (ISP + Galangin group): demonstrating a moderate amount of collagen fibers in the endomysium (arrows). (M.T. × 200) (H6) A histogram displaying the mean area percentage of collagen fibers.

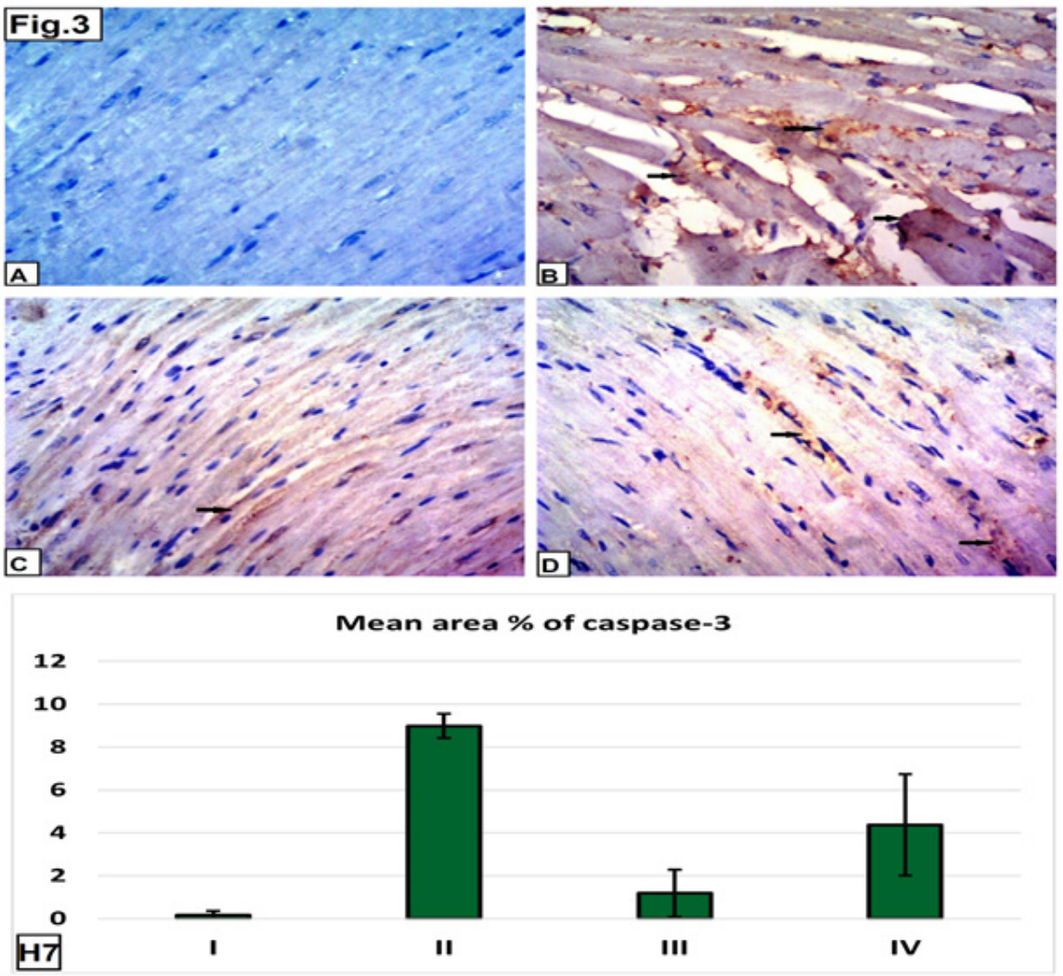

Fig. 3: A photomicrograph of a longitudinal section of the myocardium: (A) Group I: demonstrating negative sarcoplasmic immune expression. (B) Group II (ISP group): displaying a strong positive sarcoplasmic immunological reactivity (arrows). (C) Group III (ISP + G-CSF group): demonstrating mild positive sarcoplasmic immune expression (arrows). (D) Group IV (ISP + Galangin group): demonstrating moderate positive sarcoplasmic immune expression(arrows). (Caspase-3 × 200) (H7) A histogram illustrating the mean area percentage of Caspase-3 immunostaining.

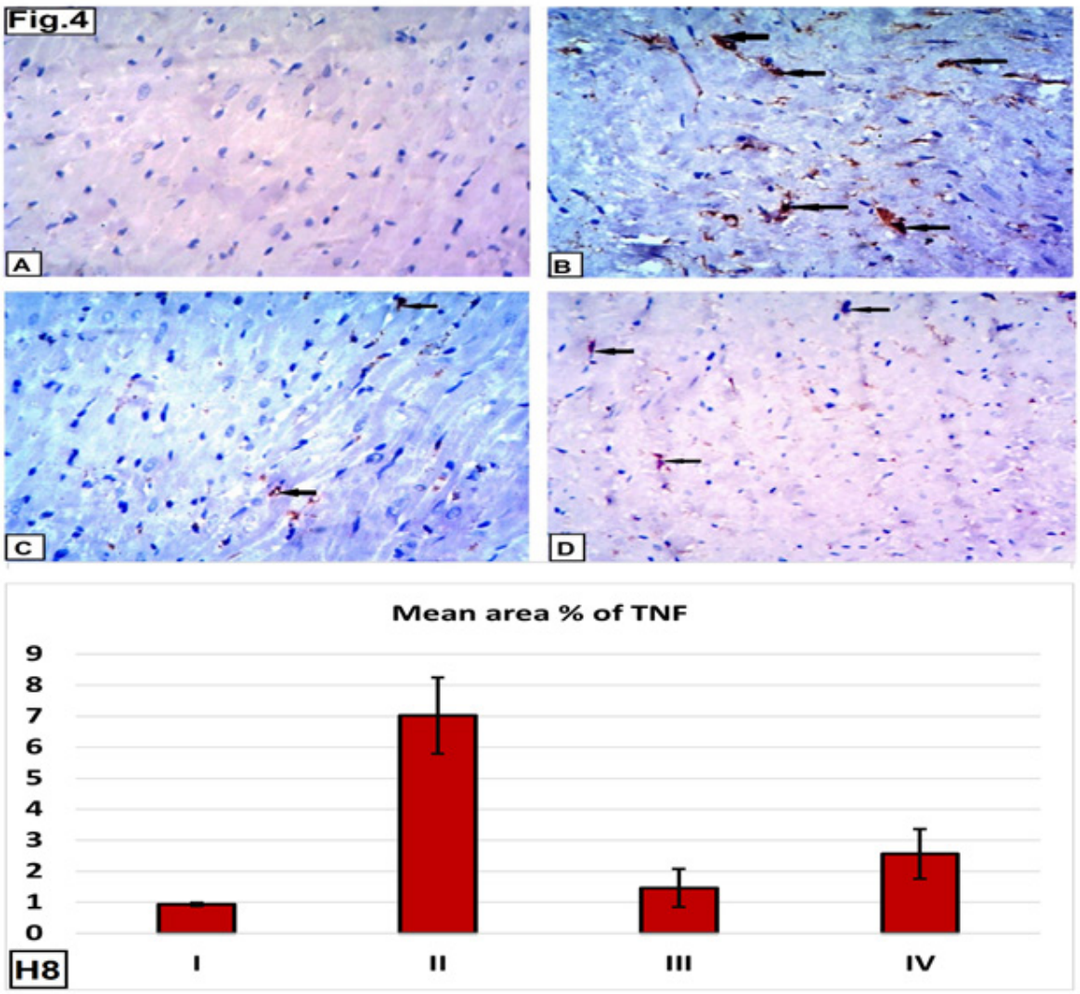

Fig. 4: A longitudinal section of the myocardium (A) Group I: displaying negative immune expression for TNF-α. (B) Group II (ISP group) revealing a strong positive nuclear immunological reactivity (arrows) for TNF-α. (C) Group III (ISP + G-CSF group): demonstrating mild positive nuclear immune expression (arrows). (D) Group IV (ISP + Galangin group): demonstrating moderate positive nuclear immune expression (arrows). (TNF-α × 200) (H8) Histogram illustrating the mean area percentage of TNF-α immune expression.

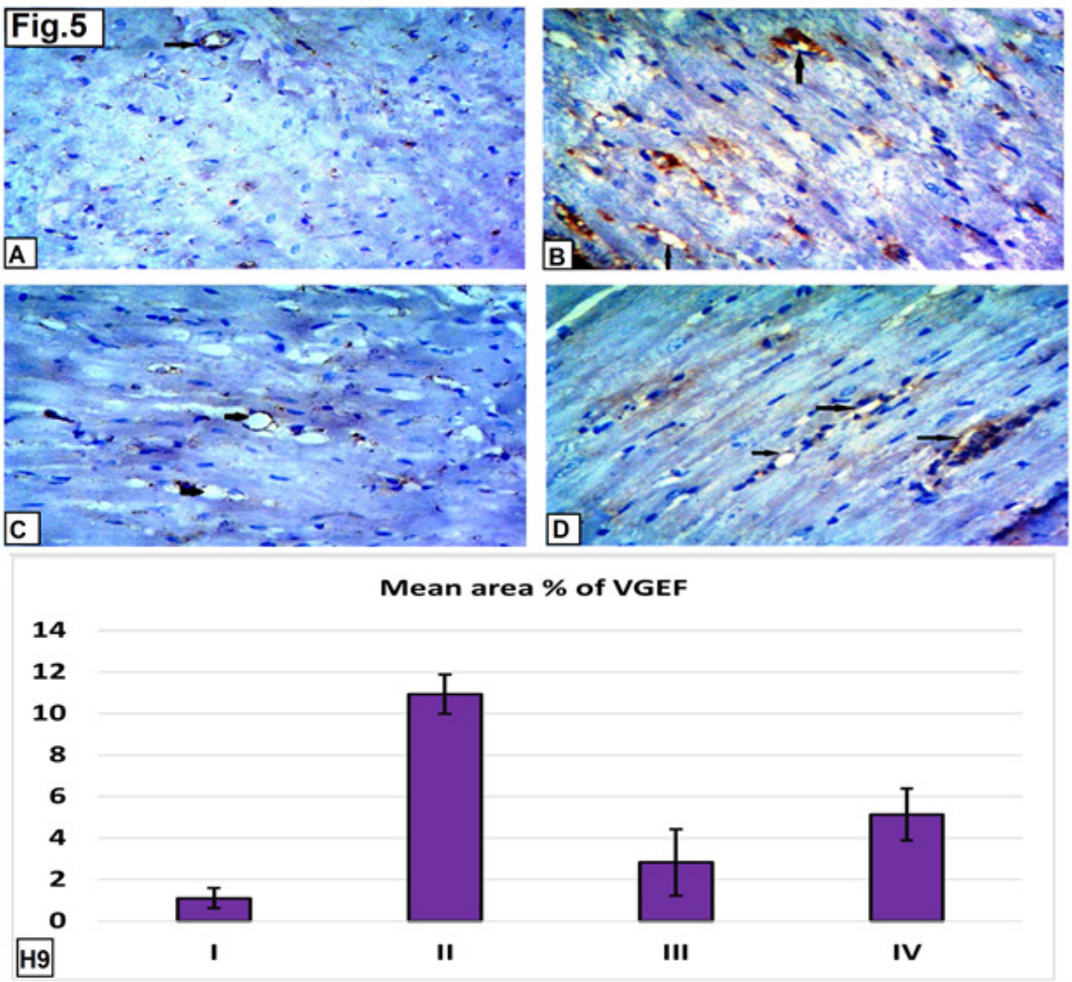

Fig. 5: A longitudinal section of the myocardium (A) (Control group) revealing a minimal positive cytoplasmic immunoreaction for VEGF in endothelial cells lining blood vessels. (B) Group II (ISP group): demonstrating a strong positive immunoreaction for (VEGF). (C) Group III (ISP + G-CSF group): exhibiting slight positive VEGF immunoreactivity (arrows). (D) Group IV (ISP + Galangin group): showing moderate positive VEGF immunoreaction (arrows). (Anti-VEGF immunostaining x 200) (H9) A histogram illustrating the mean area percentage of VEGF immunoreaction.

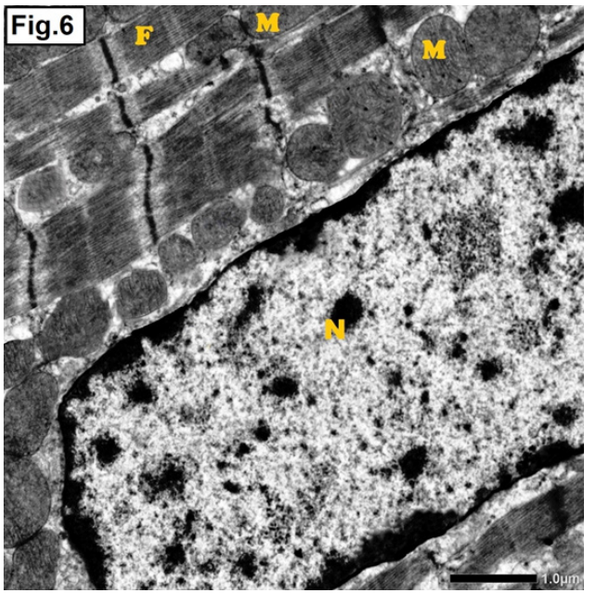

Fig. 6: An electron photomicrograph of a cardiomyocyte from the control group with euchromatic nucleus (N) surrounded by normal myofibrils (F). Mitochondria (M) are found between the myofibrils and around the nucleus. (TEM × 5000)

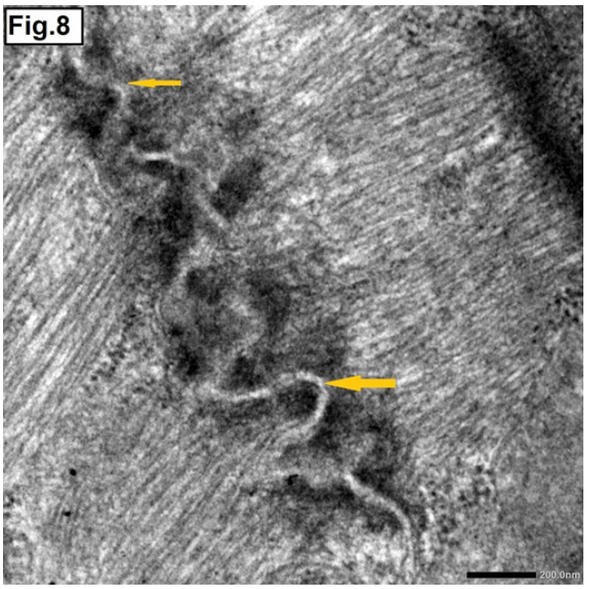

Fig. 8: An electron photomicrograph of two cardiomyocytes from control rats, separated by an apparently normal intercalated disc (arrow). (TEM × 20000)

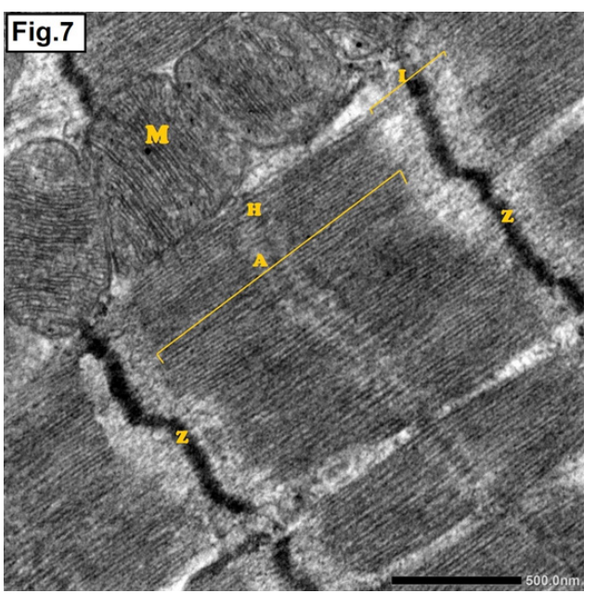

Fig. 7: An electron photomicrograph from the control group (group I) cardiomyocyte reveals parallel rays of regularly distributed myofibrils with alternating light I bands (I) bisected by the Z-line (Z) and dark A bands (A) bisected by the H-zone. Mitochondria (M) are seen. (TEM × 15000)

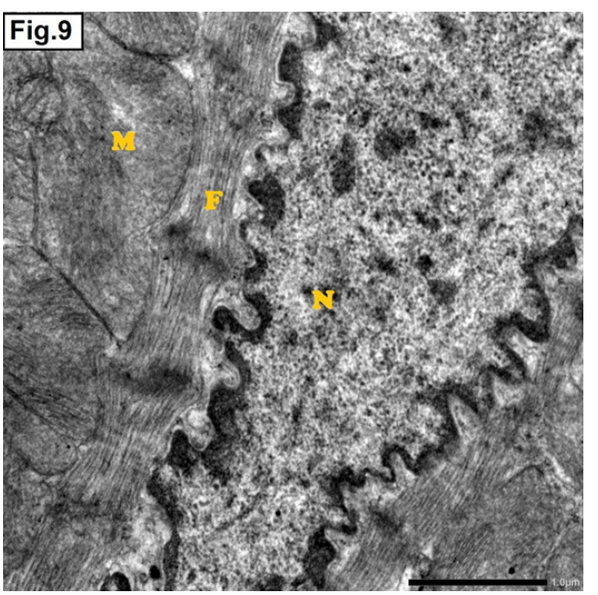

Fig. 9: An electron photomicrograph of a cardiomyocyte in Isoprotrenol-treated group (II) reveals an irregularly indented nucleus (N) with peripherally condensed marginated chromatin. Swollen mitochondria (M) and disruptions in the banding pattern of myofibrils (F) are also observed. (TEM × 8000)

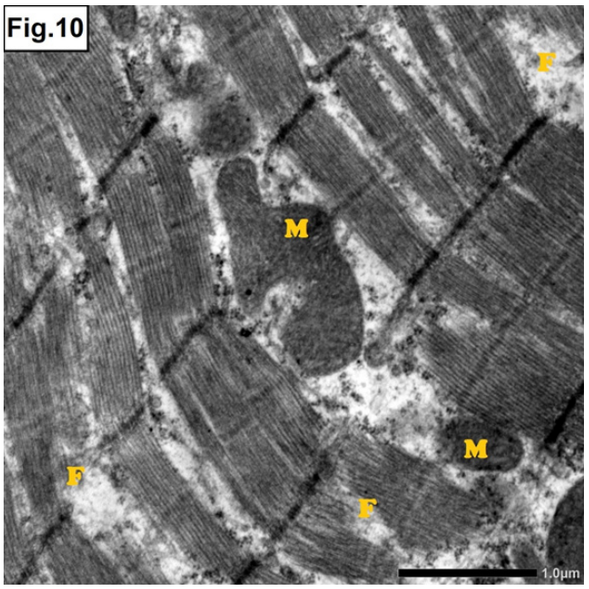

Fig. 10: An electron photomicrograph of a cardiomyocyte from the Isoprotrenol-treated group (II) shows fragmentation and disruption of the myofibril banding pattern (F), as well as mitochondrial damage (M). (TEM × 8000)

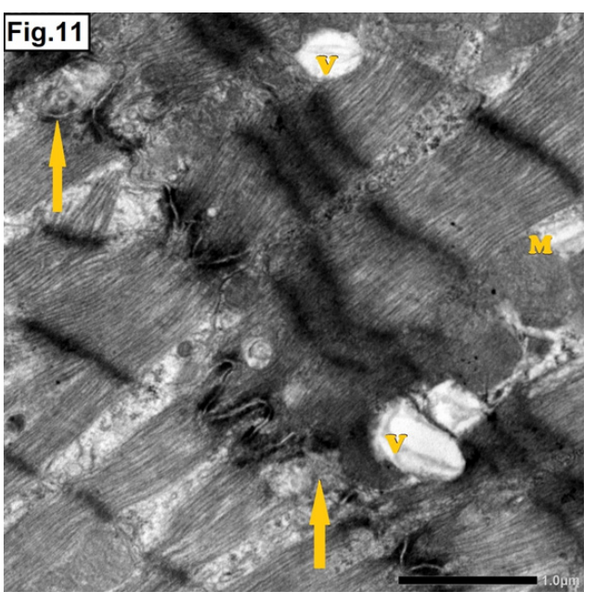

Fig. 11: An electron photomicrograph of a cardiomyocyte from the Isoprotrenol-treated group (group II) shows disruption of the usual myofibril pattern as well as degeneration (F). There are vacuoles (V), a deformed intercalated disc (arrow), and damaged mitochondria (M). (TEM×8000)

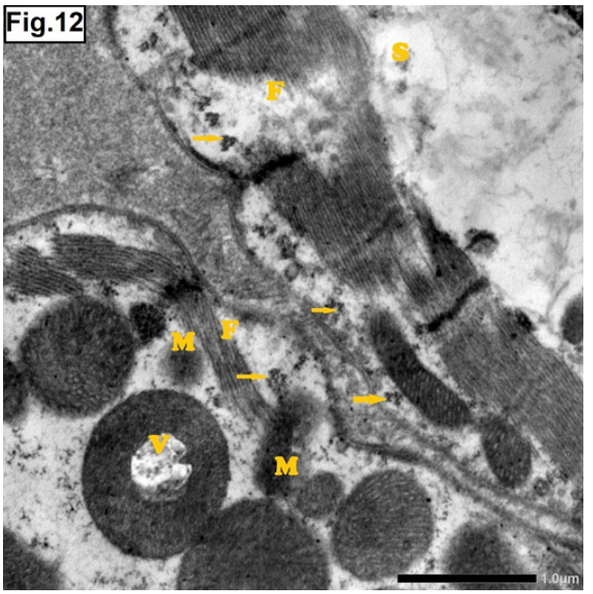

Fig. 12: An electron photomicrograph of the Isoprotrenol-treated cardiomyocyte (group II) shows a loss of normal myofibril pattern and arrangement, with some myofibrils having degenerated patches (F) and others exhibiting full lysis(S). The mitochondria are damaged (M), resulting in the formation of a central vacuole(V). Notice the abundance of glycogen granules (arrows) between the degraded myofibrils. (TEM × 8000)

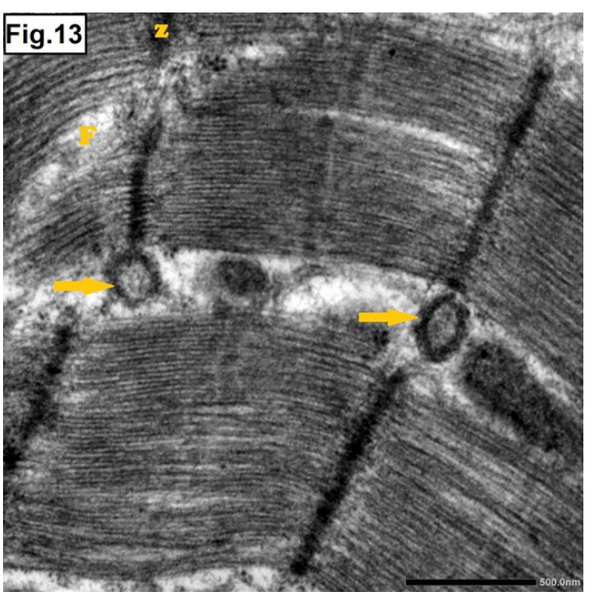

Fig. 13: An electron photomicrograph of the Isoprotrenol-treated cardiomyocyte (group II) shows degraded myofibrils (F), T-tubule dilatation (arrow), and an interrupted Z-line patch. (TEM × 15000)

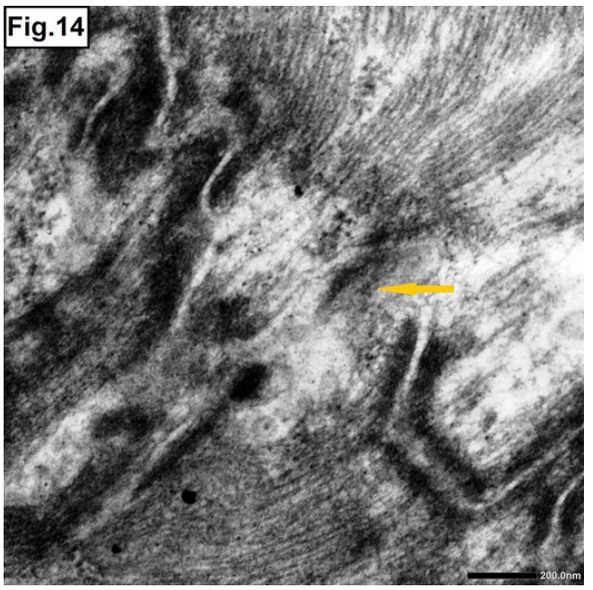

Fig. 14: An electron photomicrograph of Isoprotrenol-treated cardiomyocyte (group II) shows significant disruption of the intercalated disc (arrow) and extensive myofibril degeneration (F). (TEM × 20000)

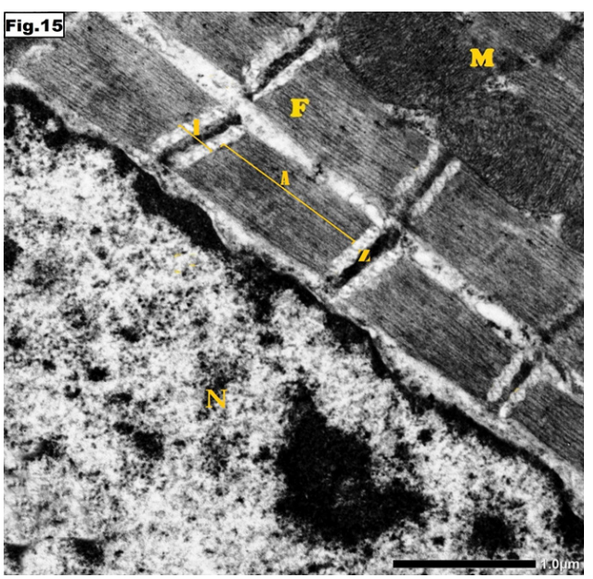

Fig. 15: An electron photomicrograph of a cardiomyocyte from the Isoprotrenol and GCSF-treated group (III) displays a euchromatic nucleus (N), nearly regularly arranged myofibrils (F), and dark A (A) and bright I (I) bands. I bands appear to be divided by Z lines (Z). Moreover, a row of mitochondria (M). (TEM × 8000)

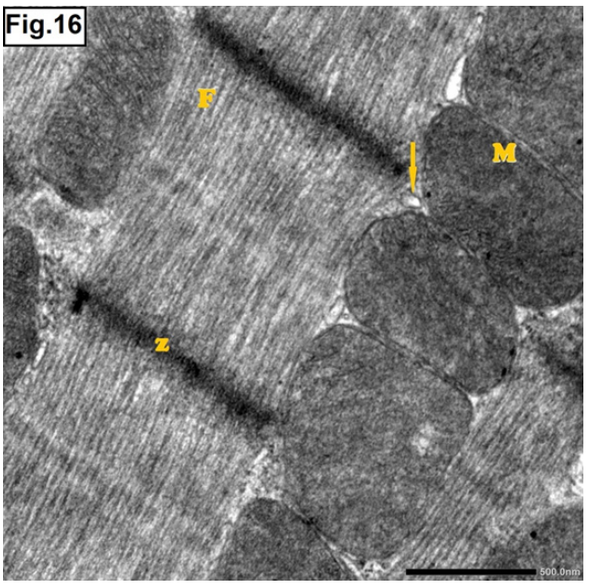

Fig. 16: An electron photomicrograph of a cardiomyocyte treated with Isoprotrenol and GCSF (III) reveals rows of myofibrils (F) separated by rows of mitochondria. Z-lines (Z) are clearly apparent. Examine the T-tubule in its usual form (arrow). (TEM × 15000)

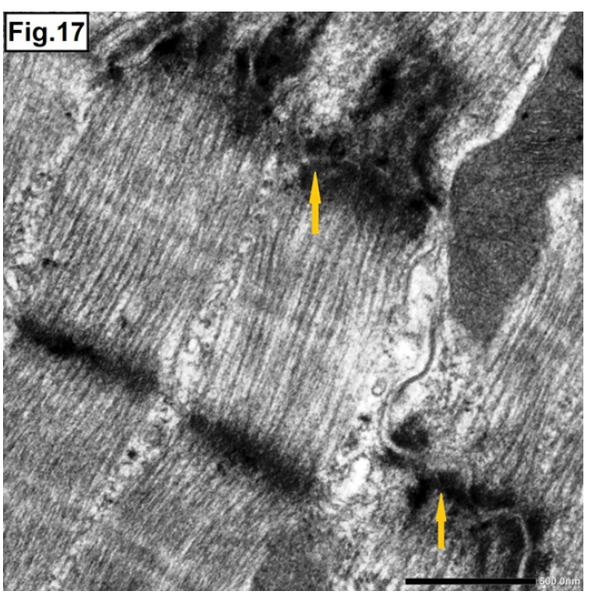

Fig. 17: An electron photomicrograph of a cardiomyocyte from the Isoprotrenol and GCSF-treated group displaying an intact intercalated disc (arrow). (TEM × 20000)

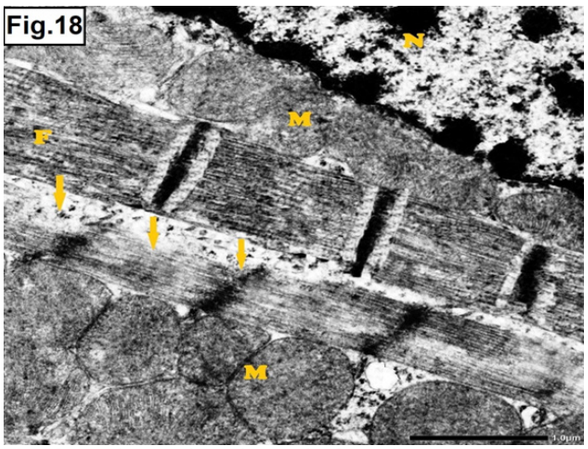

Fig. 18: An electron photomicrograph of a cardiomyocyte treated with Isoprotrenol and Galangin (IV) shows an irregularly indented nucleus with peripherally condensed chromatin (N) and nearly regularly distributed myofibrils (F); there are areas of degeneration in myofibrils and Z-lines (arrows). Mitochondria (M) in the perinuclear region and surrounding myofibrils. (TEM × 8000)

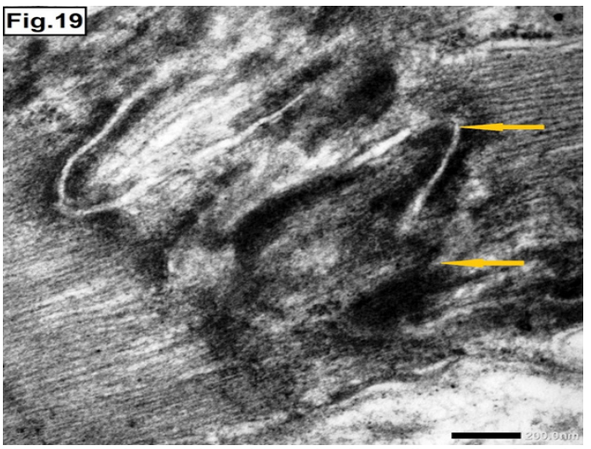

Fig. 19: An electron photomicrograph of a cardiomyocyte from the Isoprotrenol and Galangin-treated group (IV) reveals an intercalated disc with distorted patches (arrows). (TEM × 20000)

Table 1: The statistical means (X) and standard deviations (SD) of the different experimental groups' body weight (gm),heart weight (gm) andCardiac Serum Marker Enzymes.

Parameters	means (X) and standard deviations (SD)				*P value*
	Group I	Group II	Group III	Group IV	
Body weight	195.33±2.4	172.35±1.3	189.14±11.2	180.83±6.6	P1=0.0001 P2=0.21 P3=0.001 P4=0.005 P5=0.01 P6 =0.12
Ht weight	0.730 ± 0.03	0.967 ±0.08	0.800±0.03	0.876 ± 0.04	P1=0.0001 P2=0.06 P3=0.0001 P4= 0.001 P5 = 0.003 P6 =0.078
CTn (ng/ml)	0.55±0.07	2.35±0.56	0.80±0.27	1.52±0.7	P1=0.000 P2=0.060 P3=0.005 P4=0.0001 P5= 0.04 P6=0.03
CK-MB(U/L)	70.69±2.96	141.79± 3.97	77.054± 5.86	86.64± 4.11	P1=0.0001 P2=0.62 P3=0.001 P4= 0.001 P5=0.001 P6 =0.02
LDH(U/L)	150.082±0.62	230.07± 29.6	163.320± 14.78	182.17± 13.76	P1=0.0001 P2=0.053 P3=0.0002 P4= 0.001 P5= 0.01 P6 =0.045

P value>0.05: non-significant. *P value*<0.05: significant. *P value*<0.001: highly significant

P_1= comparisonwas done between ISP treated group (group IV) and control group (group I).

P_2= comparisonwas done between ISP and G-CSF treated group (group V) and control group (group I).

P_3= comparisonwas done between ISP and Galangin treated group (group VI) and control group (group I).

P_4= comparisonwas done between ISP and G-CSF treated group (group V) and ISP treated group (group IV).

P_5= comparisonwas done between ISP and Galangin treated group (group VI) and ISP treated group (group IV).

P_6= comparisonwas done between and ISP and GCSF treated group (group V)and ISP and Galangin treated group (group VI).

Table 2: Statistical Comparison between different studied groups as regardslipid peroxidation enzyme (MDA) and antioxidant enzymes (glutathione, SOD and CAT).

Parameters	means (X) and standard deviations (SD)			*P value*	
	Group I	Group II	Group III	Group IV	
MDA (n mol/mg ptn)	41.75±1.53	134.86 ±11.8	53.07±13.1	73.42 ± 11.7	P1=0.0001 P2=0.06 P3=0.001 P4=0.002 P5=0.001 P6=0.018
Glutathione (Mmol/mg ptn)	10.53±0.39	6.88±1.8	9.91±0.6	8.78±1.01	P1=0.0006 P2=0.08 P3=0.003 P4=0.0004 P5=0.042 P6=0.047
SOD (U/mg ptn)	6.63±0.25	3.78±1.4	6.08±0.91	5.17± 0.36	P1=0.0008 P2=0.17 P3=0.003 P4=0.008 P5=0.046 P6=0.046
CAT (U/mg ptn)	14.68±0.32	7.65±3.03	14.033±0.97	11.45±2.22	P1=0.0002 P2=0.14 P3=0.005 P4=0.001 P5=0.03 P6=0.026

P value>0.05: non-significant. *P value*<0.05: significant. *P value*<0.001: highly significant

P_1= comparisonwas done between ISP treated group (group IV) and control group (group I).

P_2= comparisonwas done between ISP and G-CSF treated group (group V) and control group (group I).

P_3= comparisonwas done between ISP and Galangin treated group (group VI) and control group (group I).

P_4= comparisonwas done between ISP and G-CSF treated group (group V) and ISP treated group (group IV).

P_5= comparisonwas done between ISP and Galangin treated group (group VI) and ISP treated group (group IV).

P_6= comparisonwas done between and ISP and GCSF treated group (group V)and ISP and Galangin treated group (group VI).

Table 3: Statistical means and standard deviations of area percentageof collagen fibers and TNF-α (±SD), VEGF and Caspase-3 (±SD) in all studied groups.

Parameters	means (X) and standard deviations (SD)			*P value*	
	Group I	Group II	Group III	Group IV	
Mean area % of collagen fibers	2.44 ± 0.16	8.17±2.31	3.21± 0.9	4.96 ± 1.52	P1=0.0001 P2=0.07 P4= 0.0006 P3=0.002 P5= 0.02 P6=0.04
Mean area % of TNF-α	0.93 ± 0.05	7.02 ± 1.23	1.46± 0.61	2.56± 0.8	P1=0.0001 P2=0.06 P3=0.001 P4= 0.0004 P5= 0.002 P6=0.024
Mean area % of VEGF immunostaining	1.10± 0.48	10.93± 0.94	2.83± 1.6	5.13±1.24	P1=0.0001 P2=0.051 P3=0.001 P4= 0.001 P5= 0.003 P6=0.035
Mean area% of Caspase-3 immunostaining	0.170±0.19	8.99± 0.57	1.19± 1.1	4.37±2.36	P1=0.0001 P2=0.08 P3=0.004 P4= 0.001 P5= 0.003 P6=0.03

P value>0.05: non-significant. *P value*<0.05: significant. *P value*<0.001: highly significant

P_1= comparisonwas done between ISP treated group (group IV) and control group (group I).

P_2= comparisonwas done between ISP and G-CSF treated group (group V) and control group (group I).

P_3= comparisonwas done between ISP and Galangin treated group (group VI) and control group (group I).

P_4= comparisonwas done between ISP and G-CSF treated group (group V) and ISP treated group (group IV).

P_5= comparisonwas done between ISP and Galangin treated group (group VI) and ISP treated group (group IV).

P_6= comparisonwas done between and ISP and GCSF treated group (group V)and ISP and Galangin treated group (group VI).

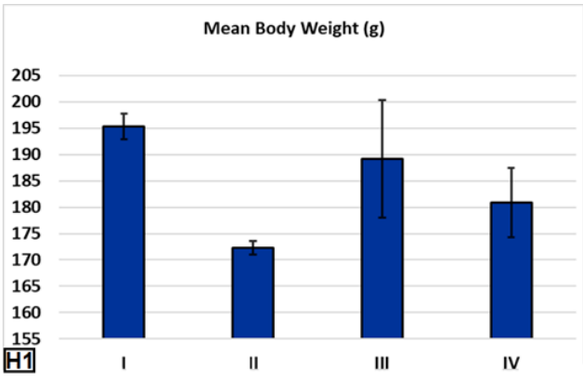

Histogram 1: illustrates mean body weight in grams

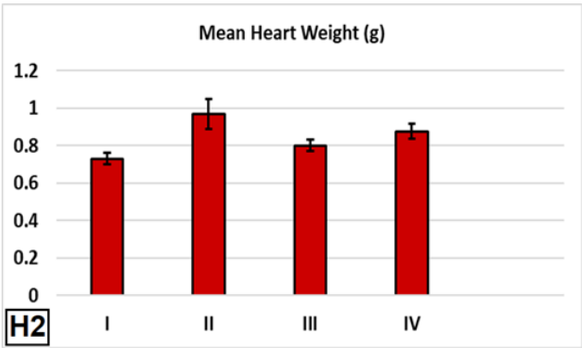

Histogram 2: illustrates mean heart weight in grams

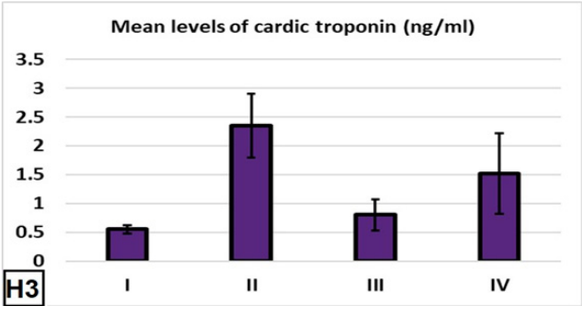

Histogram 3: illustrates mean cardiac troponin level (ng/ml)

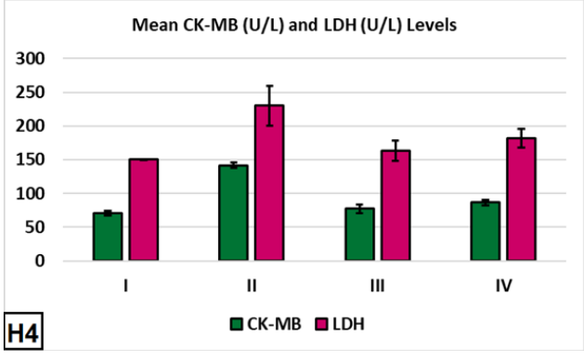

Histogram 4: illustrates mean creatine kinase -MB (CK-MB) (U/L), and lactate dehydrogenase (LDH)(U/L) levels

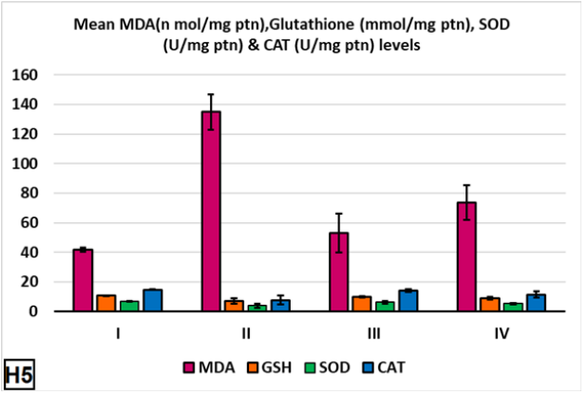

Histogram 5: illustrates mean Malondialdehyde (MDA) (nmol/mg), Reduced glutathione (GSH) (mmol/mg protein), Superoxide dismutase (SOD) (U/mg protein), and Catalase (CAT) (U/mg protein) levels

DISCUSSION

A myocardial infarction (MI), frequently referred to as a heart attack, is a serious clinical disease characterized by an insufficient blood supply to the myocardium. Myocardial infarction causes myocardial injury or necrosis[2]. ISP-induced myocardial ischemia is a straightforward, cost-effective, non-invasive, and time-saving MI model that involves minimal surgery and preserves the pericardium. ISP administration often causes cardiac dysfunction and left ventricular dilatation like the extensively infarcted heart[16].

Isoproterenol and G-CSF or galangin were investigated for cardiac function improvement. Stem cell treatment may mend the heart. By improving heart function and avoiding ventricular remodeling, stem cell transplantation improves CIHD patients' prognosis. G-CSF-mediated mobilization of bone marrow-derived progenitor cells provides a less intrusive method to tissue repair[30].

In the current study, the group which received ISP had lost body weight and gained heart weight. Jain *et al*.[31] discovered that increasing water content, congestion, swollen intramuscular space, extensive cardiac muscle necrosis subsequent to inflammatory cellular infiltration of the injured tissue, and protein content may all raise heart weight, whereas decreasing food intake could reduce body weight. Cardiovascular troponin (cTn I), creatine kinase MB isoenzyme (CK-MB), and lactate dehydrogenase (LDH) are established MI markers. The mean serum levels of CK-MB, cTn I, and LDH increased significantly in our study with rats treated with ISP than normal rats. Our results had similarities with prior investigations[4,32], which reported that ISP-treated rats had considerably greater serum LDH and cTnI levels than controls. According to Jain *et al*.[31], ISP's cardiotoxic effects cause myocardial necrosis, causing necrotic myocytes to leak cardiac enzymes into the circulation. This refers to the main cause of elevated levels after cell membrane rupture. An enhanced cell membrane permeability, DNA alterations, and cell death from lipid peroxidation can cause aging, sickness, and other impairments[33,34].

Several disorders, including MI, depend on lipid peroxidation. In this work, ISP therapy significantly increased plasma MDA levels, indicating lipid peroxidation and oxidative stress. In addition, this group lowered GSH, SOD, and CAT, the enzymes that best protect against free radical-induced oxidative stress. Galal *et al*.[35] reported that ISP-treated tissue had greater MDA levels than the control group, while Dianita *et al*.[36] found that isoproterenol decreased GPx, CAT, and SOD levels. Isoproterenol (ISP) causes cardiotoxicity by increasing oxidative stress in cardiac tissue, which depletes antioxidant enzymes, according to Allawadhi *et al*.[37], ISP depletes oxygen, causing cardiac hypoxia and necrosis. Increasing lipid peroxidation causes cellular permeability and cardiac enlargement.

ISP generates cytotoxic free radicals and reactive oxygen species. This process upsets the delicate state of equilibrium of free radicals and antioxidant defense mechanisms, like human myocardial infarction (MI)[38]. Ahmed *et al*.[6] informed that ISP-induced Ca2+ influx is a major cause of cardiac dysfunction and myocardial injury.

This study found cardiac muscle architecture degradation in light microscopic sections of the ISP-treated group's left ventricular myocardium. Wavy appearance of cardiac fibers with areas of complete loss, and dark pyknotic nuclei are noticed. Expansion of the endomysium caused extravasation and severe bleeding. Acidophilic exudate, vacuolation, and cellular invasion were seen. Shukla *et al*.[16] and Jain *et al*.[31] found deteriorated myocardium, nuclear pyknosis, edema, vacuole formation, inflammation, and muscle fibrosis in ISP-treated patients. These were explained as isoproterenol enhanced ROS generation, affecting cellular activity and inducing rat heart necrosis. Damaged areas produce superoxide radicals from isoproterenol[39]. ISP-induced injury to the myocardium was caused by elevated heart rate (HR), and infarct size according to Nwokocha *et al*.[40].

Mallory's trichrome-stained myocardial slices from rats treated with ISP exhibited increased endomysium and blood vessel collagen. In contrast to the control group, the ISP group displayed a high mean collagen fiber area. ISP-treated rodents had increased left atrial fibrosis. corroborating Ma *et al*.[41]. Yang *et al*.[42] linked ISP to increased cardiac tissue collagen types I and III expression and α-SMA synthesis. Myofibroblasts, which express contractile proteins including α-SMA, are transformed from cardiac fibroblasts. Cardiac fibrosis was worsened by ISP treatment, which increased hydroxyproline, matrix metalloproteinases 2 and 9, and collagen-I protein more than the control[43].

ISP-treated rats had higher myocardial Caspase-3 immunoreactivity and mean area percentage than controls. This mirrored previous investigations[44,45]. ISP alone upregulated cardiac tissue caspase-3, the main apoptotic protein[46]. Oxidative stress destabilizes mitochondria and lysosomes, strains the endoplasmic reticulum, activates pro caspases, releases pro-apoptotic chemicals into the cytoplasm, and promotes cardiac cell death, causing heart failure[4].

The ISP-treated group showed a strong nuclear response to TNF-α through immunohistochemistry labeling. A considerable increase in ISP-treated rats contrasted with control group, which was validated morphometrically, indicating severe inflammation. Previous research[47] found increased TNF-α immune-expression in the ischemia group, affecting monocyte activation, cytokine release, remodeling and fibrosis via TNFR1. TNF-a may cause sepsis and heart damage. When TNF-a starts the inflammatory cascade, vascular endothelial cells' cytokines, chemokines, and adhesion molecules boost neutrophil adherence[48].

The ISP-treated group had higher VEGF cytoplasmic immunoreaction than controls that was validated morphometrically by a highly significant increase in its mean area percentage in relation to control animals. This was supported by Zaitone and Abo-Gresha[49], who showed higher VEGF levels and immunostaining in isoproterenol-treated rats' cardiac tissues. Ischemic diseases may benefit from angiogenesis. Angiogenesis compensates for ischemic tissues by sustaining cardiac blood flow[50]. Hypoxia provokes the release of growth factors such as VEGF, which promotes emerging and capillary expansion within ischemic tissues. This adapts vascular density to growth and physiological oxygen demand[51].

The ISP-treated rats' heart muscle electron microscopy exhibited an irregularly indented nucleus, peripherally condensed marginated chromatin, damaged swollen mitochondria with central vacuole, and myofibril banding disruption. Full lysis and a large perinuclear sarcoplasmic gap between myofibrils and nuclei. Broken Z-lines and tubule dilatation were also, found. The intercalated disk was poorly structured. These results were coincided with Huwait[52] who found altered sarcomere broken myocardium, and damaged mitochondria, heart mitochondrial hypertrophy, or uneven shape. Isoproterenol-treated myocytes showed ultrastructural damage with myofibril loss, minimal mitochondrial enlargement, and condensed nucleus chromatin, as did Sharma *et al*.[53]. Isoproterenol inhibiting AMPK may cause ER stress, cardiac cell damage, BNP release, apoptosis, and heart failure[54]. G-CSF treatment for myocardial infarction and ischemic heart disease is less intrusive and better[10].

The average serum levels of cTnI, CK-MB, and LDH were calculated. Unlike the ISP-treated group, the ISP and GCSF-treated group exhibited considerably lower serum cardiac enzyme levels. Abdelrahman *et al*.[10] discovered that GCSF dramatically lowered AST, LDH, and CK-MB. Ren *et al*.[55] found significant LDH reduction after G-CSF injection.

The ISP and GCSF treatment group indicated substantially decreased plasma MDA concentrations than the ISP group, but increased serum glutathione, SOD,

and catalase levels and activity. Hou *et al*.[56] discovered that G-CSF dramatically reduced MDA and raised GSH in heart, kidney, and liver tissues. Abdel Mohsen *et al*.[57] found that G-CSF reduced MDA and lipid peroxidation improved myelin regeneration in spinal cord and brain injuries. G-CSF's antioxidant activity reduced ROS generation, mitochondrial membrane potential changes, and edema from cisplatin-induced cerebellar injury.

The isoproterenol and G-CSF groups' left ventricular wall myocardial light microscopic sections showed almost complete restoration of the usual structure with centrally located, pale oval vesicular nuclei. Flattened fibroblast nuclei, intercalated discs connect cardiomyocytes were found. In ischemic rats, GCSF enhanced myocardial regeneration, according to Hassan *et al*.[58]. G-CSF reduces myocardial cell death and increases local angiogenesis in ischemic areas to enhance left ventricular systolic performance, damage, and perfusion[55].

Mallory's trichrome-stained sections of rats treated with ISP and GCSF exhibited significant cardiac collagen fiber area reduction. Liu *et al*.[59] observed G-CSF reduces myocardial fibrosis. Li *et al*.[60] found reduced fibrosis in G-CSF and vildagliptin-treated rats. G-CSF activates MMP-2 and MMP-9. El-Haroun *et al*.[9] found that G-CSF inhibits TGF-β1 expression and produces anti-fibrogenic cytokines, leading to decreased collagen deposition. G-CSF lowered TGF-b1 and IL-6 mRNA levels.

Caspase-3 immunohistochemistry in GCSF and isoproterenol rats' myocardium showed a moderate sarcoplasmic immunological response. Taşkıran *et al*.[61] found reduced caspase-3 immuno-expression in GCSF and Doxorubicin groups in their study. These findings may be attributable to G-CSF's anti-inflammatory and anti-apoptotic properties[62]. G-CSF protects oligodendrocytes from spinal cord injury-induced cell death by reducing inflammatory cytokines and increasing anti-apoptotic protein[63]. Park *et al*.[64] observed that G-CSF reduces cardiomyocyte apoptosis and improves cardiac function in diabetic cardiomyopathy. ER stress-induced death factors like caspase-9 and caspase-12 were decreased by G-CSF.

This study found a significant decrease in TNF-α area % in myocardial sections of GCSF and ISP-treated groups. Kadota *et al*.[63] reported that GCSF decreases pro-inflammatory cytokine (IL-1 beta and TNF-α) expression at mRNA and protein levels.

VEGF immunohistochemistry showed slight positive cytoplasmic staining with myocardial sections of GCSF and ISP treated rats similar to that of control group. This was confirmed morphometrically with no statistical difference to control group. G-CSF induces cardiac expression of angiogenic factors in *vitro* and in *vivo*. This may promote angiogenesis and protect against endothelial apoptosis by producing angiogenic factors, preventing cardiomyocyte cell death and cardiac remodeling after myocardial infarction and increase myelomonocytic cells[65,66].

Ultrastructural analysis of G-CSF-treated cardiomyocytes showed the euchromatic nucleus, homogeneous myofibrils with normal mitochondrial arrangement, and dark A and light I bands alternation. Myocardium contained normal T-tubules and intact intercalated discs. G-CSF's anti-fibrotic and anti-apoptotic activities enhanced most cardiac muscle fiber ultrastructure, according to Abdelrahman *et al*.[10].

G-CSF reduces myocardial mitochondrial swelling, membrane potential, and ROS. G-CSF may protect cardiac mitochondria from oxidative stress[67]. Previous studies have shown G-CSF's therapeutic effects on the liver, kidney, spinal cord, brain lesions, and irradiated salivary glands[62,68]. D'Amario *et al*.[69] found that G-CSF caused bone marrow cells to form cardiomyocytes in infarcted mouse hearts. G-CSF mobilization reduces infarctions, improves blood circulation, protects myocardium, and delays ventricular remodeling. G-CSF reduced collagen deposition by generating anti-fibrogenic cytokines and lowering TGF-1 expression, as did El-Haroun *et al*.[9]. These findings highlight the necessity to balance G-CSF's anti-angiogenic, anti-fibrosis, immunosuppressive, and anti-apoptotic properties with its atherosclerotic and inflammation-causing adverse effects[17].

This trial showed that Galangin and ISP benefited heart tissue, but not enough. Co-administration of ISP and Galangin reduced cardiac troponin (c Tn I), CK-MB, and LDH significantly in comparison to the ISP-treated group as Thangaiyan *et al*.[14] confirmed. MDA plasma levels were significantly lower in ISP and Galangin groups. Ravichandra *et al*.[70] found that Galangin treatment may slightly lower MDA levels by reducing lipid peroxidation.

ISP and Galangin treated animals had dramatically reduced glutathione, SOD, and catalase levels and activity. In agreement with this result, other researchers[14] revealed that Galangin treatment significantly reduced ISP-induced loss of enzymatic antioxidants (CAT, SOD and GPx) in rat RBCs and heart tissue. This cardioprotection property of Galangin might be due to its antioxidant property. GA has several structural motifs which are responsible for its antioxidant potential such as C-2-C-3 double bond and a C-3 hydroxyl bond. Moreover, GA has the ability to scavenge free radicals like superoxide and singlet oxygen[14].

Left ventricular wall myocardial sections of ISP and galangin treated group normalized relatively. However, Pyknotic nuclei, expanded endomysium, vacuoles, and hemorrhagic areas were identified. This was supported by Abukhalil *et al*.[71] who stated that galangin corrected histological abnormalities in most cardiac fibers with mild degeneration in diabetic rats. Galangin established its cardioprotective action in rats by lowering infiltration of inflammatory cells and maintaining the structure of the heart muscle fibers[72].

In cardiac sections of rats treated with galangin and ISP, endomysium collagen increased somewhat. Through enhanced TGF-1 expression, Thangaiyan *et al*.[14] found that

GA inhibited ISP-induced interstitial collagen synthesis in the heart using Masson's trichrome staining.

A modest sarcoplasmic immunological response was seen in rats' myocardium when Caspase-3 was immunostained. Yu *et al*.[72] found that galangin treatment reduced apoptosis by increasing Bcl2 and decreasing Bax. In diabetic rats, galangin lowers Bax and Caspase-3 and enhances cardiac Bcl-2[71].

TNF-α and Vascular endothelial growth factor (VEGF) immunohistochemistry for rats' myocardium of ISP and Galangin treated group showed a significant moderate positive nuclear and cytoplasmic immunological expression. TNF-α levels were significantly reduced after GA pretreatment[14]. Galangin dose-dependently reduced angiogenesis by downregulating VEGF[73]. Furthermore, the anti-inflammatory properties of Galangin supported by reductions in heart and systemic TNF- α and IL-6 concentrations, may augment its favorable effects on the heart[11].

Electron microscopy showed irregularly indented nuclei with peripherally condensed chromatin and almost regularly dispersed myofibrils in this group's cardiomyocytes, but Z-line degeneration persisted. Rows of mitochondria surrounded myofibrils as well as perinuclei and warped intercalated discs existed. Tomar *et al*.[74] found that Galangin treatment with cisplatin caused less nucleus deformation and fewer vacuoles. Galangin decreases oxidative stress, preserves cell membranes, and improves heart systolic/diastolic dysfunction. It also, decreased systemic and tissue oxidative stress and boosted antioxidant activity, while lower doses had no effect[75].

Concluding our investigation, the efficacy of the myocardium protection offered by the combination of G-CSF and isoproterenol was more effective than that of Galangin. Despite this, Galangin maintained its efficacy. G-CSF is a highly potent medication that safeguards the heart against any potential damage that could affect it. We advocate clearly for further investigation into the potential applications of Galangin and G-CSF in the treatment of a broad variety of pathological conditions.

Based on this evaluation, the following recommendations are crucial. More research is needed to determine the protective effects of G-CSF and Galangin and on humans. Further research is required to determine the optimal G-CSF and Galangin dosage for greatest benefit while minimizing risks.

CONFLICT OF INTERESTS

There are no conflicts of interest.

REFERENCES

1. Rhana, P.; Barros, G.M.; Oliveira Santos, V.C.; Costa, A.D.; Santos, D.M.; Fernandes-Braga, W. & *et al*., (2022): "S-limonene protects the heart in an experimental model of myocardial infarction induced by isoproterenol: Possible involvement of mitochondrial reactive oxygen species". European Journal of Pharmacology. Volume 930, 2022, 175134. https://doi.org/10.1016/j.ejphar.2022.175134.
2. Jenča, D., Melenovský, V., Stehlik, J., Staněk, V., Kettner, J., Kautzner, J., Adámková V. & Wohlfahrt, P. (2021): "Heart failure after myocardial infarction: incidence and predictors". ESC heart failure, 8(1), 222-37. https://doi.org/10.1002/ehf2.131443
3. Fathima, S. N. (2021): "An Update on Myocardial Infarction. Current Research and Trends in Medical Science and Technology", 1(1):1-33.
4. Khalifa, A. A., Rashad, R. M., & El-Hadidy, W. F. (2021): "Thymoquinone protects against cardiac mitochondrial DNA loss, oxidative stress, inflammation and apoptosis in isoproterenol-induced myocardial infarction in rats". Heliyon, 7(7) e07561. https://doi.org/10.1016/j.heliyon.2021.e07561.
5. Abo Raya, A.A.; Ibrahim, M.A.A. & Qureshi, H. A. (2017): "Role of Different Doses of Vitamin E in Protection Against Isoproterenol-Induced Myocardial Damage in Adult Male Albino Rat: A Light and Electron Microscopic Study". Egyptian journal of histology. 40(2), 129-40. https://dx.doi.org/10.21608/EJH.2017.4072
6. Ahmed, M.I; Abdelrazek, H.M.A; Moustafa, Y.M; Alshawwa, S.Z; Mobasher, M.A; Abdel-Wahab, B.A. & *et al*., (2023): "Cardioprotective Effect of Flibanserin against Isoproterenol-Induced Myocardial Infarction in Female Rats: Role of Cardiac 5-HT2A Receptor Gene/5-HT/Ca2+ Pathway". Pharmaceuticals. 16(4):502. https://doi.org/10.3390/ph16040502
7. Theyab, A.; Algahtani, M.; Alsharif, K. F.; Hawsawi, Y. M.; Alghamdi, A. & Akinwale, J. (2021): "New insight into the mechanism of granulocyte colony-stimulating factor (G-CSF) that induces the mobilization of neutrophils". Hematology, 26(1), 628-36. https://doi.org/10.1080/16078454.2021.1965725
8. Wicks, I. P. & Roberts, A. W. (2016): "Targeting GM-CSF in inflammatory diseases". Nature Reviews Rheumatology, 12(1), 37-48. https://doi.org/10.1038/nrrheum.2015.161.
9. El-Haroun, H., Bashandy, M. A. & Soliman, M. A. E. (2022): "Impact of Remdesivir on the kidney and potential protective capacity of Granulocyte-Colony Stimulating Factor versus Bone Marrow Mesenchymal Stem Cells in adult male albino rats". Egyptian Journal of Histology, 45(2), 338-58. https://dx.doi.org/10.21608/ejh.2021.60527.1426
10. Abdelrahman, S. A.; Khattab, M. A.; Youssef, M. S. & Mahmoud, A. A. (2023): "Granulocyte-colony stimulating factor ameliorates di-ethylhexyl phthalate-induced cardiac muscle injury via stem cells recruitment, Desmin protein regulation, antifibrotic and antiapoptotic mechanisms". Journal of Molecular Histology, (54):349-63. https://doi.org/10.1007/s10735-023-10137-6.

11. Prasatthong, P.; Meephat, S.; Rattanakanokchai, S.; Khamseekaew, J.; Bunbupha, S.; Prachaney, P. & *et al*., (2021): Galangin Resolves Cardiometabolic "Disorders through Modulation of AdipoR1, COX-2, and NF-κB Expression in Rats Fed a High-Fat Diet". Antioxidants (Basel, Switzerland), 10(5): 769. https://doi.org/10.3390/antiox10050769.

12. Mosa, O.F. (2021): "Beneficial role of Galangin on gentamicin-induced nephrotoxicity in rat model: A Pharmaco-biochemical study". Life Science Journal. 18 (5): 9-15. http://www.lifesciencesite.com 2.doi:10.7537/marslsj180521.02.

13. Wu, B., Xu, C., Ding, H. S., Qiu, L., Gao, J. X., Li, M., Xu H. & Liu, X. (2022): "Galangin inhibits neointima formation induced by vascular injury via regulating the PI3K/AKT/mTOR pathway". Food & Function, 13(23), 12077-92. https://doi.org/10.1039/D2FO02441A

14. Thangaiyan, R.; Arjunan, S.; Govindasamy, K.; Khan, H. A.; Alhomida, A. S. & Prasad, N. R. (2020): "Galangin attenuates isoproterenol-induced inflammation and fibrosis in the cardiac tissue of albino wistar rats". Frontiers in Pharmacology, 11, 585163. DOI=10.3389/fphar.2020.585163.

15. Aloud, A.A.; Veeramani, C.; Govindasamy, C.; Alsaif, M.A.; El Newehy, A.S. & Al-Numair, K.S. (2017): "Galangin, a dietary flavonoid, improves antioxidant status and reduces hyperglycemia-mediated oxidative stress in streptozotocin-induced diabetic rats". Redox Rep. Commun. Free Radic. Res., 22, 290–300. https://doi.org/10.1080/13510002.2016.1273437.

16. Shukla, S. K., Sharma, S. B., & Singh, U. R. (2015): "β-Adrenoreceptor agonist isoproterenol alters oxidative status, inflammatory signaling, injury markers and apoptotic cell death in myocardium of rats". Indian journal of clinical biochemistry, 30, 27-34. https://doi.org/10.1007/s12291-013-0401-5.

17. Huang, R.; Lv, H.; Yao, K.; Ge, L.; Ye, Z.; Ding H., & *et al*. (2018): "Effects of different doses of granulocyte colony-stimulating factor mobilization therapy on ischemic cardiomyopathy". Sci Rep.; 8(1),5922. https://doi.org/10.1038/s41598-018-24020-y

18. Wellington, D.; Mikaelian, I. & Singer, L. (2013): "Comparison of ketamine-xylazine and ketamine-dexmedetomidine anesthesia and intraperitoneal tolerance in rats" J. Am. Assoc. Lab. Anim. Sci. 52(4):481-87.

19. Radhiga, T.; Rajamanickam, C.; Senthil, S. & Pugalendi, K.V. (2012): "Effect of ursolic acid on cardiac marker enzymes, lipid profile and macroscopic enzyme mapping assay in isoproterenol-induced myocardial ischemic rats". Food Chem. Toxicol. 50(11): 3971-7. https://doi.org/10.1016/j.fct.2012.07.067.

20. Milinković-Tur, S.; Aladrović, J.; Beer Ljubić, B. & Poljičak-Milas, N. (2009): "Age-related antioxidant enzyme activities and lipid peroxidation in heart muscles of broiler chickens fed with supplementary organic selenium". Veterinarski Arhiv, 79(5), 481-9.

21. Zammel, N.; Saeed, M.; Bouali, N.; El-kahoui, S.; Alam, J.M.; Rebai, T.; Kausar, M.A.; Adnan, M.; Siddiqui, A.J. & Badraoui, R. (2021): "Antioxidant and Anti-Inflammatory Effects of Zingiber officinale roscoe and Allium subhirsutum". In Silico, Biochemical and Histological Study. Foods. 10(6):1383. https://doi.org/10.3390/foods10061383.

22. Shaikh, S.; Bhatt, L. K. & Barve, K. (2019): "Attenuation of isoproterenol-induced cardiotoxicity in rats by Narirutin rich fraction from grapefruit". Phytomedicine, 55, 222-8. https://doi.org/10.1016/j.phymed.2018.06.037.

23. Ganesan, B.; Buddhan, S.; Anandan, R.; Sivakumar, R. & AnbinEzhilan, R. (2010): "Antioxidant defense of betaine against isoprenaline-induced myocardial infarction in rats". Mol Biol Rep. (37)1319-27. https://doi.org/10.1007/s11033-009-9508-4.

24. Kiernan J.A. (2015): "Histological and histochemical methods: Theory and practice, 5th edition in special stains and Hx & E": Folia Histochemica ET Cytobiologica; 54(1):58–9.

25. Kaushal, V., Herzog, C., Haun, R. S., & Kaushal, G. P. (2014): "Caspase protocols in mice. In: V. Bozhkov, P., Salvesen, G. (eds) Caspases, Paracaspases, and Metacaspases. Methods in Molecular Biology", vol 1133. Humana Press, New York, NY. 141-54. https://doi.org/10.1007/978-1-4939-0357-3_9.

26. Jammal, M. P., Araújo da Silva, A., Martins Filho, A., de Castro Côbo, E., Adad, S. J., Murta, E. F. C., & Nomelini, R. S. (2015): "Immunohistochemical staining of tumor necrosis factor-α and interleukin-10 in benign and malignant ovarian neoplasms". Oncology letters, 9(2), 979-83. https://doi.org/10.3892/ol.2014.2781.

27. Kamar, S. S., Abdel-Kader, D. H., & Rashed, L. A. (2019): "Beneficial effect of Curcumin Nanoparticles-Hydrogel on excisional skin wound healing in type-I diabetic rat: Histological and immunohistochemical studies". Annals of Anatomy-Anatomischer Anzeiger, 222, 94-102. https://doi.org/10.1016/j.aanat.2018.11.005.

28. Tizro, P.; Choi, C., & Khanlou, N. (2019): "Sample Preparation for Transmission Electron Microscopy". In: Yong, W. (eds) Biobanking. Methods in Molecular Biology, (33): 417-24. Humana Press, New York, NY. https://doi.org/10.1007/978-1-4939-8935-5_33.

29. Barton, B. & Peat, J (2014):" Medical statistics, A Guide to SPSS data analysis and critical appraisal" 2nd ed., BMJ books-Blackwell.5:112-35.

30. Hu, Z.; Chen, Z.; Wang, Y.; Jiang, J.; Tse, G.; Xu, W.; Junbo G & Sun, B. (2019): "Effects of granulocyte colony stimulating factor on rabbit carotid and porcine heart models of chronic obliterative arterial disease" Molecular Medicine Reports, 19(6), 4569-78. https://doi.org/10.3892/mmr.10120.

31. Jain, P. G.; Mahajan, U. B.; Shinde, S. D. & Surana, S. J. (2018): "Cardioprotective role of FA against isoproterenol induced cardiac toxicity". Molecular biology reports, 45, 1357-65. https://doi.org/10.1007/s11033-018-4297-2.

32. Asaikumar, L., Vennila, L., Akila, P., Sivasangari, S., Kanimozhi, K., Premalatha, K., & Sinhu, G. (2020): "Preventive effect of nerolidol on isoproterenol induced myocardial damage in Wistar rats": Evidence from biochemical and histopathological studies (Expression of Concern of Vol 80, Pg 814, 2019). Drug development research, 81(5), 638. https://doi.org/10.1002/ddr.21564.

33. Su, L. J., Zhang, J. H., Gomez, H., Murugan, R., Hong, X., Xu, D., Jiang, F.& Peng, Z. Y. (2019): "Reactive oxygen species-induced lipid peroxidation in apoptosis, autophagy, and ferroptosis". Oxidative medicine and cellular longevity, Article ID 5080843. 1-13, https://doi.org/10.1155/2019/5080843.

34. Iuchi, K., Takai, T., & Hisatomi, H. (2021): "Cell death via lipid peroxidation and protein aggregation diseases". Biology, 10(5), 399. https://doi.org/10.3390/biology10050399.

35. Galal, O., Mostafa, A., Mohamed, H., Ahmed, A. R., Hashim, M. S., & Mohamed, N. (2022): "Cardioprotective Effects of Nano-Vitamin D on Isoprenaline-Induced Myocardial Infarction Rat Model." SVU-International Journal of Medical Sciences, 5(2), 136-51. https://doi.org/10.21608/svuijm.2022.131434.1301.

36. Dianita, R., Jantan, I., Amran, A. Z., & Jalil, J. (2015): "Protective effects of Labisia pumila var. alata on biochemical and histopathological alterations of cardiac muscle cells in isoproterenol-induced myocardial infarction rats". Molecules, 20(3), 4746-63. https://doi.org/10.1002/ptr.6152.

37. Allawadhi, P.; Khurana, A.; Sayed, N.; Kumari, P., & Godugu, C. (2018): "Isoproterenol-induced cardiac ischemia and fibrosis: Plant-based approaches for intervention". Phytotherapy Research, 32(10), 1908-32. https://doi.org/10.1002/ptr.6152.

38. Chaudhary, P.; Janmeda, P.; Docea, A. O.; Yeskaliyeva, B.; Abdull Razis, A. F.; Modu, B., Calina, D., & Sharifi-Rad, J. (2023): "Oxidative stress, free radicals and antioxidants: potential crosstalk in the pathophysiology of human diseases". Frontiers in chemistry, Article ID: 11:1158198. 1:24. https://doi.org/10.3389/fchem.2023.1158198.

39. Sajid, A.; Ahmad, T.; Ikram, M.; Khan, T.; Shah, A. J.; Mahnashi, M. H. & *et al*., (2022): "Cardioprotective potential of aqueous extract of Fumaria indica on isoproterenol-induced myocardial infarction in SD rats". Oxidative Medicine and Cellular Longevity, Article ID 2112956, 11 pages. https://doi.org/10.1155/2022/2112956.

40. Nwokocha, C.; Palacios, J.; Simirgiotis, M. J.; Thomas, J.; Nwokocha, M.; Young, L.; *et al*., (2017): "Aqueous extract from leaf of Artocarpus altilis provides cardio-protection from isoproterenol induced myocardial damage in rats: Negative chronotropic and inotropic effects". Journal of ethnopharmacology, 203, 163-70. https://doi.org/10.1016/j.jep.2017.03.037.

41. Ma, S., Ma, J., Tu, Q., Zheng, C., Chen, Q., & Lv, W. (2020): "Isoproterenol increases left atrial fibrosis and susceptibility to atrial fibrillation by inducing atrial ischemic infarction in rats". Frontiers in Pharmacology, 11, 493. https://doi.org/10.3389/fphar.2020.00493

42. Yang, H. X.; Xu, G. R.; Zhang, C.; Sun, J. H.; Zhang, Y.; Song, J. N.; Liu Y. & Li, A. Y. (2020): "The aqueous extract of Gentianella acuta improves isoproterenol induced myocardial fibrosis via inhibition of the TGF β1/Smads signaling pathway". International journal of molecular medicine, 45(1), 223. https://doi.org/10.3892/ijmm.2019.4410

43. Viswanadha, V. P., Dhivya, V., Beeraka, N. M., Huang, C. Y., Gavryushova, L. V., Minyaeva, N. N., Tarasov V.V. & Aliev, G. (2020): "The protective effect of piperine against isoproterenol-induced inflammation in experimental models of myocardial toxicity". European Journal of Pharmacology, 885, 173524. https://doi.org/10.1016/j.ejphar.2020.173524

44. Ismail, D. I., ShamsEldeen, A. M., Rashed, L. A., Shama, A. A. E. D., Ashour, S. S., & Aboulkhair, A. G. (2021): "Cardioprotective Potential of Zinc and Vitamin E Against Isoprenaline-Induced Myocardial Infarction in Albino Rats by Targeting Autophagy: A Histological and Biochemical Study". Egyptian Journal of Histology, 44(2), 450-64. https://dx.doi.org/10.21608/ejh.2020.36645.1331

45. Khalaf, H. M., Abdalla, A. M., Ahmed, A. F., & Abdel-Aziz, A. M. (2020): "Role of nitric oxide in mediating the cardioprotective effect of agomelatine against isoproterenol-induced myocardial injury in rats". Naunyn-Schmiedeberg's Archives of Pharmacology, 393, 1809-23. https://doi.org/10.1007/s00210-020-01860-y.

46. Okasha, E. F., & Ragab, A. M. H. (2015): "Histological, Immunohistochemical and ultrastructural study on the effect of gold nanoparticles on the left ventricular cardiac myocytes of adult male albino rat". Middle East J. Sci. Res, 23(12), 2968-82. DOI: 10.5829/idosi.mejsr.2015.23.12.10234

47. Elkattawy, H. A.; El-sayed, H. A. E.; Ebrahim, A.; Abdelwahab, O. A., & Eldesoqui, M. (2023): "Interleukin-37 has A Promising Cardioprotective Effect on Isoproterenol-Induced Myocardial Infarction". Int. J. Morphol, 41(5), 1427-38. http://dx.doi.org/10.4067/S0717-95022023000501427

48. Khodir, A. E., Ghoneim, H. A., Rahim, M. A., & Suddek, G. M. (2016):" Montelukast attenuates lipopolysaccharide-induced cardiac injury in rats". Human & experimental toxicology, 35(4), 388-97. https://doi.org/10.1177/0960327115591372.

49. Zaitone, S. A., & Abo-Gresha, N. M. (2012):" Rosuvastatin promotes angiogenesis and reverses isoproterenol-induced acute myocardial infarction in rats: role of iNOS and VEGF". European journal of pharmacology, 691(1-3), 134-42. https://doi.org/10.1016/j.ejphar.2012.06.022.

50. Lähteenvuo, J. & Rosenzweig, A. (2012):" Effects of aging on angiogenesis". Circ Res. Apr 27;110(9):1252-64. doi: 10.1161/CIRCRESAHA.111.246116. PMID: 22539758; PMCID: PMC4101916.

51. Moon, S.; Chang, M.S., Koh, S.H. & Choi, Y.K. (2021): "Repair Mechanisms of the Neurovascular Unit after Ischemic Stroke with a Focus on VEGF". International Journal of Molecular Sciences. 22(16):8543. https://doi.org/10.3390/ijms22168543.

52. Huwait, E. A. (2019): "Combination of vitamin E and L-carnitine is superior in protection against isoproterenol-induced cardiac injury: histopathological evidence". Folia Morphologica, 78(2), 274-82. https://doi.org/10.5603/FM.a2018.0070.

53. Sharma, S.; Iqubal, A.; Khan, V.; Sharma, K.; Najmi, A. K. & Haque, S. E. (2023): "Icariin ameliorates oxidative stress-induced inflammation, apoptosis, and heart failure in isoproterenol-challenged Wistar rats. Iranian Journal of Basic Medical Sciences, 26(5), 517". https://doi.org/10.22038%2FIJBMS.2023.66481.14589.

54. Zhuo, X. Z., Wu, Y., Ni, Y. J., Liu, J. H., Gong, M., Wang, X. H., Yuan Z & Song, P. (2013): "Isoproterenol instigates cardiomyocyte apoptosis and heart failure via AMPK inactivation-mediated endoplasmic reticulum stress". Apoptosis, 18, 800-10. https://doi.org/10.1007/s10495-013-0843-5.

55. Ren, P., Zhang, M., & Dai, S. (2020): "Therapeutic effects of coronary granulocyte colony-stimulating factor on rats with chronic ischemic heart disease". Open Life Sciences, 15(1), 742-52. https://doi.org/10.1515/biol-2020-0078.

56. Hou, X. W.; Jiang, Y.; Wang, L. F.; Xu, H. Y.; Lin, H. M.; He, X. Y. & *et al*., (2009):" Protective role of granulocyte colony-stimulating factor against Adriamycin induced cardiac, renal and hepatic toxicities. Toxicology letters, 187(1), 40-44. https://doi.org/10.1016/j.toxlet.2009.01.025.

57. Abdel Mohsen, A. F.; Ahmed, N. A. W.; Altaib, Z. M. & Zaher, S. M. (2020): "Effect of cisplatin on cerebellar cortex of albino rat and possible protective role of granulocyte Colony stimulating factor versus Citrullus Lanatus juice: a histological study". Egyptian journal of histology, 43(3), 702-17. https://dx.doi.org/10.21608/ejh.2019.19193.1197.

58. Hassan, G. M., El-Wazir, Y. M., Ahmed, N. S., & Farage, A. E. (2010): "Effect of CD34+ Stem Cell Injection and their Mobilization from Bone Marrow by Granulocyte-Colony Stimulating Factor in Regeneration of Myocardium after Experimental Induction of Acute Myocardial Infarction in Adult Albino Rat". Suez Canal University Medical Journal, 13(1), 1-6. https://dx.doi.org/10.21608/scumj.2010.69753

59. Liu, L., Zhang, J., & Wei, X. (2018): "Effects of combined MCA and G-CSF treatment on myocardial fibrosis and apoptosis gene expression in rats with diastolic heart failure". Int J Clin Exp Med, 11(2), 1352-61. https://e-century.us/files/ijcem/11/2/ijcem0059616.

60. Li, M.; Wang, Z.; Xia, H.; Yu, L. & Hu, Z. (2019): "Vildagliptin and G-CSF improved angiogenesis and survival after acute myocardial infarction". Archives of Medical Research, 50(3), 133-41. https://doi.org/10.1016/j.arcmed.2019.07.004.

61. Taşkıran, E., Erdoğan, M. A., Yiğittürk, G., & Erbaş, O. (2019): "Therapeutic effects of liraglutide, oxytocin and granulocyte colony-stimulating factor in doxorubicin-induced cardiomyopathy model: an experimental animal study". Cardiovascular Toxicology, 19, 510-17.

62. Khorasanizadeh, M.; Eskian, M.; Vaccaro, A. R., & Rahimi-Movaghar, V. (2017): "Granulocyte colony-stimulating factor (G-CSF) for the treatment of spinal cord injury". CNS drugs, 31, 911-37. https://link.springer.com/article/10.1007/s40263-017-0472-6.

63. Kadota, R., Koda, M., Kawabe, J., Hashimoto, M., Nishio, Y., Mannoji, C. & *et al*., (2012): "Granulocyte colony-stimulating factor (g-csf) protects oligpdendrocyte and promotes hindlimb functional recovery after spinal cord injury in rats". PloS one, 7(11), e50391. https://doi.org/10.1371/journal.pone.0050391.g001.

64. Park, I.H.; Shen, G.Y.; Song, Y.S.; Jong, C. Y.; Kim B.S.; Lee, Y. & *et al*., (2021): "Granulocyte colony-stimulating factor reduces the endoplasmic reticulum stress in a rat model of diabetic cardiomyopathy". Endocr J. Nov 29;68(11):1293-301. doi: 10.1507/endocrj. EJ21-0016. Epub 2021 Jun 11. PMID: 34121048.

65. Harada, M.; Qin, Y.; Takano, H.; Minamino, T.; Zou, Y.; Toko, H. & *et al*., (2005): "G-CSF prevents cardiac remodeling after myocardial infarction by activating the Jak-Stat pathway in cardiomyocytes". Nature medicine, 11(3), 305-11. https://doi.org/10.1038/nm1199.

66. Ohki, Y., Heissig, B., Sato, Y., Akiyama, H., Zhu, Z., Hicklin, D.J., Shimada, K., Ogawa, H., Daida, H., Hattori, K. and Ohsaka, A. (2005): "Granulocyte colony-stimulating factor promotes neovascularization by releasing vascular endothelial growth factor from neutrophils". FASEB. J.; 19: 2005–7. https://doi.org/10.1096/fj.04-3496fje.

67. Thummasorn, S., Kumfu, S., Chattipakorn, S., & Chattipakorn, N. (2011): "Granulocyte-colony stimulating factor attenuates mitochondrial dysfunction induced by oxidative stress in cardiac mitochondria". Mitochondrion, 11(3), 457-66. https://doi.org/10.1016/j.mito.2011.01.008

68. Engelmann, C.; Herber, A.; Franke, A.; Bruns, T.; Reuken, P.; Schiefke, I. &*et al*., (2021): "Granulocyte-colony stimulating factor (G-CSF) to treat acute-on-chronic liver failure: A multicenter randomized trial (GRAFT study)". Journal of Hepatology, 75(6), 1346-54. https://doi.org/10.1016/j.jhep.2021.07.033.

69. D'Amario, D., Leone, A. M., Borovac, J. A., Cannata, F., Siracusano, A., Niccoli, G., & Crea, F. (2018): "Granulocyte colony-stimulating factor for the treatment of cardiovascular diseases: An update with a critical appraisal". Pharmacological research, 127, 67-76. https://doi.org/10.1016/j.phrs.2017.06.001.

70. Ravichandra, V., Hanumantharayappa, B., & Papasani, V. (2014): "Evaluation of cardio protective activity of galangin against doxorubicin induced cardiomyopathy". Int J Pharm Pharm Sci, 6(9), 86-90.

71. Abukhalil, M. H.; Althunibat, O. Y.; Aladaileh, S. H.; Al-Amarat, W.; Obeidat, H. M.; Alayn'Al-mar, H. O., & *et al*., (2021): "Galangin attenuates diabetic cardiomyopathy through modulating oxidative stress, inflammation and apoptosis in rats". Biomedicine & Pharmacotherapy, 138, 111410. https://doi.org/10.1016/j.biopha.2021.111410.

72. Yu, S.; Gong, L. S.; Li, N. F.; Pan, Y. F. & Zhang, L. (2018): "Galangin (GG) combined with cisplatin (DDP) to suppress human lung cancer by inhibition of STAT3-regulated NF-κB and Bcl-2/Bax signaling pathways". Biomedicine & Pharmacotherapy, (97):213-24. https://doi.org/10.1016/j.biopha.2017.10.059

73. Chen, D., Li, D., Xu, X. B., Qiu, S., Luo, S., Qiu, E. & *et al*., (2019): "Galangin inhibits epithelial-mesenchymal transition and angiogenesis by downregulating CD44 in glioma". Journal of Cancer, 10(19), 4499–508. https://doi.org/10.7150/jca.31487.

74. Tomar, A.; Vasisth, S.; Khan, S. I.; Malik, S.; Nag, T. C.; Arya, D. S. & Bhatia, J. (2017): "Galangin ameliorates cisplatin induced nephrotoxicity in *vivo* by modulation of oxidative stress, apoptosis and inflammation through interplay of MAPK signaling cascade". Phytomedicine, (34):154-61. https://doi.org/10.1016/j.phymed.2017.05.007.

75. Chaihongsa, N.; Maneesai, P.; Sangartit, W.; Rattanakanokchai, S.; Potue, P.; Khamseekaew, J. & *et al*., (2022): "Cardiorenal dysfunction and hypertrophy induced by renal artery occlusion are normalized by galangin treatment in rats". Biomedicine & Pharmacotherapy, 152, 113231. https://doi.org/10.1016/j.biopha.2022.113231.

الملخص العربى

دراسة هستولوجية و هستوكيميائية مناعية لمقارنة التأثيرات الوقائية المحتملة لعامل تحفيز مستعمرة المحببات مقابل الجالانجين على السمية القلبية المستحثة في ذكور الجرذان البيضاء

هالة محمد الحرون[١،٢]، نادية سعيد بدوي[١]، ايمان بدوي حامد[١]، منى عبد المولى سليمان[١]

[١]قسم الانسجة وبيولوجيا الخلية ـ كلية الطب ـ جامعة المنوفية

[٢]قسم العلوم الطبية الأساسية، كلية طب الأسنان، جامعة الريادة للعلوم والتكنولوجيا

المقدمة: يتميزاعتلال عضلة القلب بتغيرات هستولوجية وكيميائية حيوية ، ويساهم بشكل كبير في ارتفاع معدلات الوفيات العالمية ، و خاصة احتشاء البطين.

الهدف من البحث: تقييم التغيرات الهستولوجية بعضلة القلب الناجمة عن الايزوبروتيرنول و كذلك اكتشاف الفوائد المحتملة لعامل تحفيزمستعمرة المحببات مقابل الجالانجين

المواد والطرق: تم تقسيم ستة و ستين جرذاً بالغاً من ذكور الجرذان البيضاء عشوائيا إلى أربع مجموعات، المجموعة الأولى وظفت كمجموعة ضابطة و عددها ١٨ جرذا، المجموعة الثانية (المجموعة المعالجة بالايزوبروتيرنول) و عددهم ١٦ جرذا و تم معالجتها بجرعة ٥ مجم/كجم من وزن الجسم يوميا لمدة ١٤ يوما، المجموعة الثالثة (المجموعة المعالجة بالايزوبروتيرنول وعامل تحفيز مستعمرة المحببات GCSF) و عددهم ١٦ جرذا و تم معالجتها بالايزوبروتيرنول بالجرعة السابقة و عامل تحفيز مستعمرة المحببات(GCSF) بجرعة ١٠ ميكروجرام / كجم من وزن الجسم يوميا لمدة ستة أيام عن طريق الحقن تحت الجلد. المجموعة الرابعة (المجموعة المعالجة بالايزوبروتيرنول و الجالانجين) و عددهم ١٦ جرذا و تم معالجتها بالايزوبروتيرنول بالجرعة السابقة و الجالانجين بجرعة ١ مجم / كجم من وزن الجسم لمدة اربع اسابيع.وفى نهاية الدراسة تم تخدير الفئران وذبحهم ، والحصول على عينات القلب ومعالجتها للتقييمات الهستولوجية والهستوكيميائية المناعية وكذلك تقيمات بالمجهرالإلكتروني.

النتائج: أظهرت المجموعة المعالجة بالايزوبروترينول مستويات مرتفعة من إنزيمات القلب ، وخصوصا اللاكتات ديهيدروجينيز (LDH) ، والكرياتين كيناز (CK-MB) MB ، وتروبونين القلب (cTn I). بالإضافة إلى انخفاض مستويات الإنزيمات المضادة للأكسدة ، بما في ذلك الجلوتاثيون ، SOD ، والكاتالاز (Catalase). وأوضحت النتائج الهستولوجية فقدان عصابات الليفات العضلية ، وظهرت الانوية داكنة بالاضافة الى التسلل الخلوى و وجود نزيف فى الاندوميسيوم الذى ظهر متسعا كما زادت نسبة مساحة الكولاجين و TNF α و VEGFوCaspase -٣.

بينما أظهرت نتائج الميكروسكوب الاليكترونى وجود اضطراب وتقطيع فى الياف عضلة القلب و تلف الميتوكندريا و كذلك انكماش خط Z. بينما العلاج بعامل تحفيزمستعمرة المحببات (GCSF) أدى إلى الحفاظ على أنسجة القلب بشكل ملحوظ مقارنة بالجالانجين.

الاستنتاج: عامل تحفيز مستعمرة المحببات (GCSF) له تأثيرا وقائيا متفوقا بشكل ملحوظ فى الحفاظ على أنسجة عضلة القلب مقارنة بالجالانجين في حالات تلف عضلة القلب المستحث. ولذلك نوصى بالمزيد من الأبحاث لدراسة التأثير الوقائي للجالانجين وG-CSF على البشرمع تحديد الجرعة المثالية لـ G-CSF والجالانجين لتحقيق أكبر فائدة.